AD-A196 025

AFWAL-TR-88-1050

Precision Measurement of the Fresnel Drag Coefficient Using a Ring Laser

James G. Grote
AFWAL/AADO-2
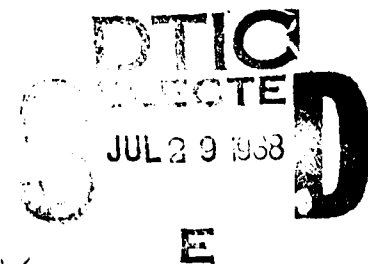Wright Patterson AFB, Ohio 45433

May 1988
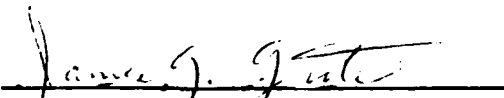**Final Report for Period Jan 1985-Sept 1986**

DTIC
ELECTE
JUL 2 9 1988
E

Avionic Laboratory
Air Force Wright Aeronautical Laboratories
Air Force Systems Command
Wright-Patterson Air Force Base, Ohio 45433

NOTICE

When Government drawings, specifications, or other data are used for any purpose other than in connection with a definitely Government-related procurement, the United Stated Government incurs no responsibility or any obligation whatsoever. The fact that the Government may have formulated or in any way supplied the said drawings, specifications, or other data, is not to be regarded by implication, or otherwise in any manner construed, as licensing the holder, or any other person or corporation; or as conveying any rights or permission to manufacture, use, or sell any patented invention that may in any way be related thereto.

This report has been reviewed by the Office of Public Affairs (ASD/PA) and is releasable to the National Technical Information Service (NTIS). At NTIS, it will be available to the general public, including foreign nations.

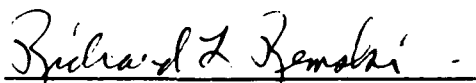This technical report has been reviewed and is approved for publication.

JAMES G. GROTE, Project Engineer
E-O Techniques & Applications Group
Electro-Optics Technology Branch

C. RICHARD LANE, Chief
E-O Techniques & Applications Group
Electro-Optics Technology Branch

FOR THE COMMANDER

RICHARD L. REMSKI, Chief
Electro-Optics Technology Branch
Electronic Technology Division

REPORT DOCUMENTATION PAGE

Form Approved
OMB No. 0704-0188

1a. REPORT SECURITY CLASSIFICATION Unclassified	1b. RESTRICTIVE MARKINGS

2a. SECURITY CLASSIFICATION AUTHORITY	3. DISTRIBUTION/AVAILABILITY OF REPORT
2b. DECLASSIFICATION/DOWNGRADING SCHEDULE	Approved for public release; distribution is unlimited.

4. PERFORMING ORGANIZATION REPORT NUMBER(S) AFWAL-TR-88-1050	5. MONITORING ORGANIZATION REPORT NUMBER(S)

6a. NAME OF PERFORMING ORGANIZATION Avionics Laboratory	6b. OFFICE SYMBOL (If applicable) AFWAL/AADO-2	7a. NAME OF MONITORING ORGANIZATION

6c. ADDRESS (City, State, and ZIP Code) WPAFB OH 45433-6543	7b. ADDRESS (City, State, and ZIP Code)

8a. NAME OF FUNDING/SPONSORING ORGANIZATION	8b. OFFICE SYMBOL (If applicable)	9. PROCUREMENT INSTRUMENT IDENTIFICATION NUMBER

8c. ADDRESS (City, State, and ZIP Code)	10. SOURCE OF FUNDING NUMBERS			
	PROGRAM ELEMENT NO.	PROJECT NO.	TASK NO	WORK UNIT ACCESSION NO.
	62204F	2001	05	07

11. TITLE (Include Security Classification)
Precision measurement of the Fresnel Drag Coefficient using a Ring laser

12. PERSONAL AUTHOR(S)
James G. Grote

13a. TYPE OF REPORT Final	13b. TIME COVERED FROM 1-85 TO 9-86	14. DATE OF REPORT (Year, Month, Day) 88/5	15. PAGE COUNT 98

16. SUPPLEMENTARY NOTATION
Thesis submitted to the University of Dayton

17. COSATI CODES			18. SUBJECT TERMS (Continue on reverse if necessary and identify by block number)
FIELD	GROUP	SUB-GROUP	Fresnel Drag Coefficient, Ring Laser Gyroscope, Fused Silica
14	02		
20	06		

19. ABSTRACT (Continue on reverse if necessary and identify by block number)

This final report is a thesis submitted to the University of Dayton. The experiment performed was a precision measurement of the Fresnel drag coefficient using a ring laser. The measurements of the parameters used to determine the Fresnel drag coefficient were significantly improved upon over previous experiments. Report covers experimental methods, procedures, measurement techniques and evaluation.

20 DISTRIBUTION/AVAILABILITY OF ABSTRACT ☒ UNCLASSIFIED/UNLIMITED ☐ SAME AS RPT ☐ DTIC USERS	21 ABSTRACT SECURITY CLASSIFICATION UNCLASSIFIED
22a NAME OF RESPONSIBLE INDIVIDUAL JAMES G. GROTE	22b TELEPHONE (Include Area Code) (513) 255-5536 — 22c OFFICE SYMBOL AFWAL/AADO-2

DD Form 1473, JUN 86   *Previous editions are obsolete*

TABLE OF CONTENTS

        History
        Fresnel Drag in a Ring Laser
        Sagnac Effect
        Determination of α

        Ring Laser Gyroscope
        Drag Site
        Computer Control

        Wavelength (λ)
        Drag Disk Thickness (l)
        Refractive Index (n) and Dispersion ($dn/d\lambda$)
        Preparation of the Drag and Compensation Disk
        Setting the Normal Angle
        Drag Disk Wobble
        Inclination Angle (β) of the Drag Disk
        Center of Rotation of the Drag Disk
        Optical Path Length (L)
        Beat Frequency and Drag Disk Rotation Rate
        and Displacement

iii

LIST OF ILLUSTRATIONS

LIST OF TABLES

ACKNOWLEDGMENT

vii

plasmas that aided in the reduction of noise in the intracavity beams. A special thanks is expressed to my wife, Camden, for her interminable and much needed support in tackling this effort.

CHAPTER I

INTRODUCTION

The intention of the research composing the content of this thesis was to improve the accuracy of the measurement of the Fresnel drag coefficient in a ring laser gyroscope, recorded by Bilger and Stowell (1977).

Fresnel drag is a change in the speed of light passing through a transparent moving medium. This change in velocity is proportional to the refractive index and velocity of the medium. The ring laser gyroscope used for this experiment was designed to test the performance characteristics of ring laser gyro mirrors. By inserting a transparent moving medium into the laser cavity, with a known index of refraction and accurately controlling its velocity, one can introduce an artificial gyro rotation rate since the output beat frequency of the ring laser gyro will be proportional to the rotation rate of the medium. Thus, it would not be necessary to rotate the ring laser itself. Measurement of the Fresnel drag coefficient was performed as a means to characterize the ring laser used for the ring laser gyro mirror investigation. Improvement in the accuracy of the drag coefficient was necessary to

1

test the performance of these laser gyro mirrors. To accomplish this, the measurement techniques for most of the parameters used to determine the drag coefficient were modified. Higher accuracy, better quality components and equipment were utilized. This resulted in accuracies in the measurements of most of the parameters exceeding or equaling those observed in the two previous experiments. The experimental apparatus were controlled and the data recorded using a computer. This provided simultaneous recording of the outputs and minimized the contribution of human error. Figure 1.1 is a photograph of the ring laser gyroscope testbed used for measuring the Fresnel drag coefficient.

The background and theoretical literature reviewed for performing this experiment is covered in Chapter II. Chapters III and IV outline the ring laser and drag site preparation and experimental techniques adopted for determining the Fresnel drag coefficient. Chapter V tabulates the data taken along with observations. The results are presented in Chapter VI. Conclusions and suggestions for improvement are given in Chapter VII. Figures are at the end of the chapters.

Figure 1.1 - Ring Laser Gyroscope Testbed and Supporting Electronics.

CHAPTER II

REVIEW OF PREVIOUS EXPERIMENTS

All major work dealing with Fresnel drag preceding this study was reviewed and will be outlined within this chapter. The main focus will be on the research performed by Bilger-Zavodny(1972) and Bilger-Stowell(1977), as the experiment undertaken was an extension of those previous works. A literature search of texts on optics and ring resonators was performed as well to support the evaluation of the parameters making up the ring laser cavity. A brief history about Fresnel drag will preclude the intended area of study.

History

Fresnel first theorized the drag effect of light through a moving refractive medium in 1818. (Lorentz, 1952).

$$\delta V_1 = [1 - (1/n^2)]V_m, \qquad\qquad 2.1$$

where $\alpha = 1 - (1/n^2)$ is Fresnel's drag coefficient, n is the refractive index of the medium at rest, δV_1 is the

velocity change of light through a transparent moving medium and V_m is the velocity of the moving medium.

Fresnel's derivation did not account for the dispersion of the material where the refractive index of the material changes with the wavelength of the propagating light. The dispersive term was included in the work performed by Lorentz in 1895. (Lorentz, 1952). He formulated

$$\alpha_{LO} = 1 - (1/n^2) - (\lambda/n)dn/d\lambda, \qquad 2.2$$

where α_{LO} is the drag coefficient given by Lorentz, λ is the wavelength of the propagating light, given in μm, and $dn/d\lambda$ is the dispersion of the medium, given in $(\mu m)^{-1}$.

Lorentz' theory best describes the situation for which the velocity V_m of the moving medium is perpendicular to the surface normal of that medium. (Parks-Dowell, 1974). See figure 2.1. For that case

$$V_i = n(\lambda)V_r, \qquad 2.3$$

where V_i is the component of V_m in the direction of the incident light and V_r is the component of V_m in the direction of the refracted light.

In 1908 Laub derived an equation for the situation in which V_m is parallel to the surface normal of the moving medium and the incident light. (Parks-Dowell, 1974).

For that case

$$V_i = V_r = V_m.$$ 2.4

Laub's equation, based on the criteria above, gives a higher order dispersive term.

$$\alpha_{La} = 1 - (1/n^2) - (\lambda/n^2)dn/d\lambda,$$ 2.5

where α_{La} is the drag coefficient given by Laub.

In 1851 Fizeau experimentally confirmed Fresnel's hypothesis using flowing water as the moving medium. (Lorentz, 1952). In 1886 Michelson and Morley repeaved Fizeau's experiment using flowing air through a pipe. (Michelson, 1962). Although both experiments demonstrated the dragging effect, the dispersive term was omitted in the comparison with theory. The dispersion term due to Laub was experimentally verified at various wavelengths by Zeeman using a moving quartz disk and glass rods translating in the direction parallel to the incident light. (Zeeman, 1914-1915). In 1964 Macek, Schneider and Salamon measured Fresnel drag using a ring laser with a quartz optical flat, dry air and CCl_4 as the solid, gas and liquid moving mediums, respectively. (Macek-Schneider-Salamon, 1964). Like the first two experiments, however, the dispersion term was also neglected in that study. Work

performed by Bilger-Zavodny was designed to measure the
dispersive term using a ring laser gyro and a fused silica
optical flat. In that experiment, V_m was perpendicular to
the surface normal predicting close comparison to the
Lorentz formula. Bilger-Zavodny claimed that the
experimental results did fit Lorentz' theory. In 1974
Parks and Dowell disputed the claim, concluding that the
results published by Bilger-Zavodny, although verifying a
dispersion term, did not provide a clear distinction
between α_{Lo} and α_{La} to within experimental error. (Parks-
Dowell, 1974). Bilger-Stowell essentially repeated the
1972 experiment but improved upon the earlier work by
further reducing the experimental error to provide the
distinction. The results published concluded that the
previous work carried out by Bilger-Zavodny had indeed
distinguished between the two dispersion terms indicating
that the drag coefficient of a moving medium in the ring
laser setup used was best modeled by the Lorentz equation.
(Bilger-Stowell, 1977).

Fresnel Drag in a Ring Laser

Starting with the equation for the beat frequency of a
ring laser with a transparent moving media in the cavity as
given by Post (1967)

$$\delta f_{Bm} = (2f/c)(\oint n^2 \alpha \overline{V} \cdot d\overline{r})/\oint n dr, \qquad 2.6$$

where δf_{Bm} is the beat frequency of the ring laser due to the moving medium, f is the frequency of the propagating beam, c is the velocity of light in a vacuum and dr is the line element along the beam path, Macek-Schneider-Salamon derived the equation

$$\delta f_{Bm} = 21V_m(n^2 - 1)/L\lambda, \qquad\qquad 2.7$$

where l is the length of the moving medium and L is the optical path length of the cavity including the moving medium.

Using the relations for drag in a rotating cylinder as presented by Bilger-Zavodny equation 2.7 becomes

$$\delta f_{Bm} = 4\pi n^2 \alpha f_m l Xo/L\lambda \tan(\beta), \qquad\qquad 2.8$$

where $f_m = V_m/2\pi$ is the rotational frequency of the moving medium, Xo is the horizontal displacement of the light beam from the axis of rotation of the moving medium and β is the angular displacement of the face of the moving medium from normal angle of incidence to the light beam. Angular displacement is about the horizontal axis. See figure 2.2 for the geometry of the experimental arrangement employed.

Sagnac Effect

Taking into account the Sagnac effect due to the

earth's rotation and adding it to equation 2.6 the total
beat frequency becomes

$$\delta f_B = \delta f_{Bm} + \delta f_{Bs}, \qquad\qquad 2.9$$

where $\delta f_{Bs} = 4A\Omega\sin(\Theta)/L\lambda$ is the beat frequency due to the
Sagnac effect realized by the rotation of the earth (Post,
1967), A is the enclosed area of the light path, Ω is the
angular velocity of the perimeter of the light path with
respect to inertial space (angular velocity of the earth)
and Θ is the angular position of the ring laser with
respect to the earth's equator (degree of latitude).[1]

The expected beat frequency due to the rotation of the
earth in the setup for this experiment is

$$\delta f_{Bs} = 78.25 \text{ Hz.}[2]$$

Determination of α

For this experiment, following the work by Bilger-
Zavodny and Bilger-Stowell, the drag coefficient will be
determined from the slope of the ratio of the beat
frequency (δf_B) to the rotational frequency of the drag

[1] $\Theta = 39^\circ$ 47' 1.5" (Official Geographic Coordinates Survey
Field Book compiled by the Wright-Patterson Air Force Base
surveyors).

[2] Including the earth's orbit, a daily peak-peak modulation
of $\delta f_{Bs} = 0.13$ Hz is expected. (Bilger-Zavodny, 1972).

disk (f_m). This is done to cancel errors due to timing of the measurements of δf_B and f_m. By connecting the time bases of the counters used to record these frequencies, any errors present in the time base will cancel when α is calculated from the slope.

$$\alpha = R(L\lambda\tan(\beta)/4\pi n^2 lXo), \qquad\qquad 2.10$$

where $R = d\delta f_B/df_m$ is the slope of the ratio of the beat frequency to the rotational frequency of the drag disk, or, $R = d\delta f_B/dXo$ is the slope of the ratio of the beat frequency to the displacement of the drag disk from the center of rotation.

The slope (R), defined by both ratios above, will be determined in this experiment for the purpose of comparison when α is evaluated.

Now, using equation 2.10, equation 2.9 can be written as

$$\delta f_B = Rf_m + \delta f_{Bs} \qquad\qquad 2.11$$

giving a general form for beat frequency.

For the experiments performed by Bilger-Zavodny and Bilger-Stowell, β was set to Brewster angle, reducing equation 2.8 to

$$\delta f_{Bm} = 4\pi n\alpha f_m 1Xo/L\lambda, \qquad\qquad 2.12$$

where $\tan(\Theta_B) = n$.

Due to the size of the disk used in this experiment, the inclination angle of the disk was not Brewster angle. See Chapter IV.
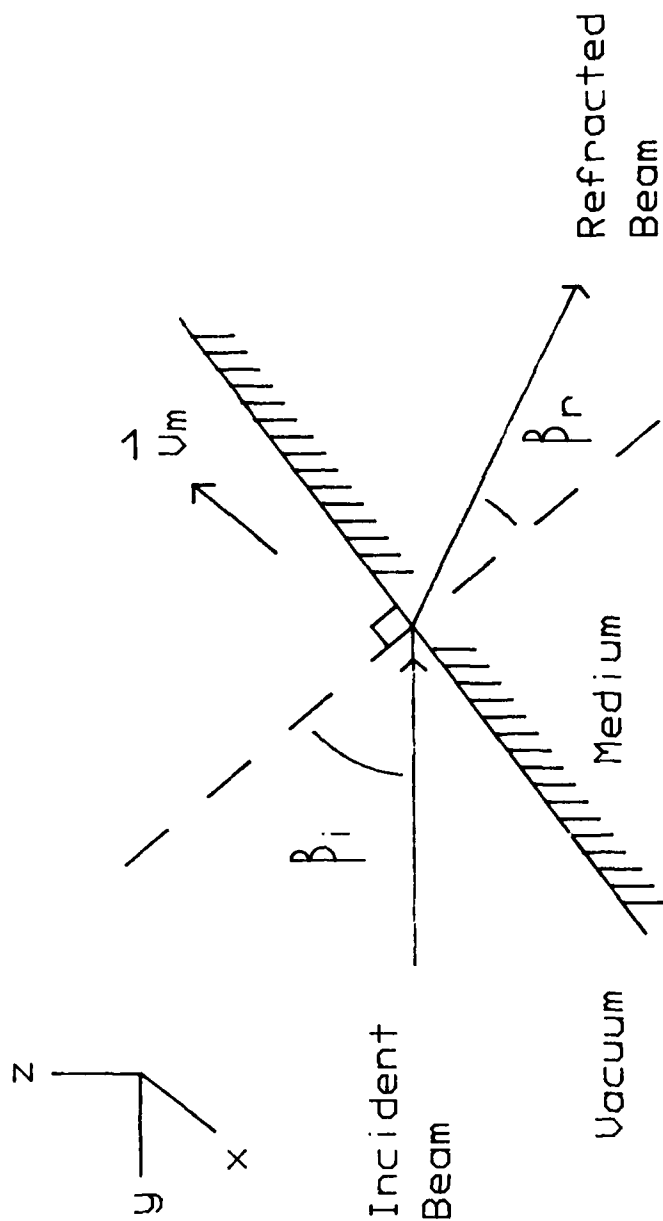
Figure 2.1 - Fresnel Drag: Illustration of Lorentz Theory.

Fused Silica
Optical Flat

f_m

β_i

β_r

CW and CCW
Laser Beams

z

x

y
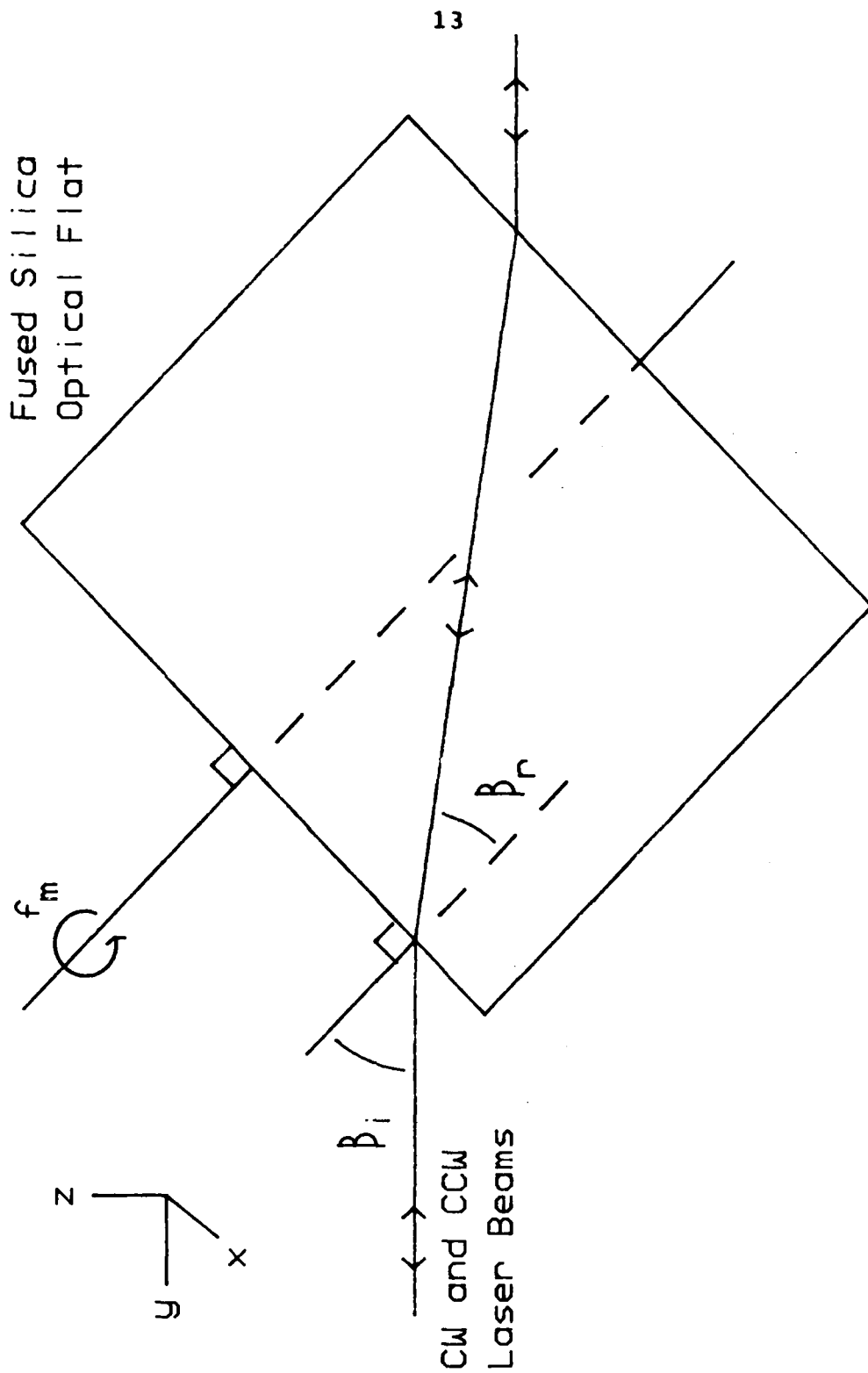
Figure 2.2 - Illustration of Drag Disk Orientation.

CHAPTER III

DRAG SITE PREPARATION AND

SUPPORTING EQUIPMENT

This chapter outlines the preparation, alignment and calibration of the equipment used in this experiment for the determination of the Fresnel drag coefficient. This includes discussion of the ring laser gyroscope and related optics, the drag site, and peripheral measurement/control equipment such as the computer and the detection systems employed.

Ring Laser Gyroscope

The configuration of the ring laser gyroscope used for this experiment was a four mirror type assembled in the shape of a square. See figure 3.1. Each leg of the ring was approximately 1 meter in length. Precise measurement of the optical path length is discussed in detail in the following chapter.

The mirror mounts and translation stages making up the ring laser were fixed to an NRC (Newport Research Corporation) model XI-45 super invar breadboard for minimum thermal expansion. See Appendix A for treatment of the

14

thermal expansion considerations. This assembly was then mounted onto a vibration isolation table specially designed by NRC to provide vibrational isolation with a 12 dB/octave rolloff in the 1 to 5 Hz range and a 24 dB/octave rolloff in the 5 to 40 Hz range.

The mirrors making up the ring laser were "S" polarized designed to have maximum reflectances at a 45° angle of incidence. Mirror M1, manufactured by Rockwell International, had a 5.75 m radius of curvature and a reflectance of 99.997%. Mirrors M2 and M4, manufactured by Northrop, had an infinite radius of curvature and a reflectance of 99.99%. Mirror M3, manufactured by OCLI (Optical Coating Laboratories, Inc.), had a 10.0 m radius of curvature and a reflectance of 99.90%. These parameters were specified by the manufacturer and were not actually measured before their use in this experiment. M3 had the lowest reflectance of the mirrors acquired and thus was used as the output mirror. The radii of curvatures of the mirrors obtained provided for a stable resonator, a beam waist radius of 0.71 mm and a beam waist length of 4.91 m with the center of the waist located at the drag disk. See Rigrod, 1965. This insured that the diameter of the beam waist would be small enough to pass through the inside diameter of the laser gain tube.

The plasma gain tube, manufactured by Jodon Engineering, was a center feed, HeNe (helium neon) with a

hot filament cathode. The plasma consisted of a special
mixture of seven parts He_3 and one part of equal quantities
of Ne_{20} and Ne_{22}. The gases in the tube were excited by
applying 13 mA at 1000 volts DC to each anode in compliance
with the manufacturers specifications by using a modified
Jodon model PS-500A plasma tube power supply. The current
through each leg was adjusted using a potentiometer and two
matched Fluke model 8020A digital multimeters to achieve a
current balance to within 0.01 mA. This was done to
minimize the directional bias of the two contrapropagating
beams. The hot filament cathode was powered with 7.0 volts
DC using an HP (Hewlett-Packard) model 6274A DC power
supply. The specifications from Jodon listed that the
filament be driven with 6.3 volts AC. Departure from this
specification was due to the high and low frequency
oscillations caused by AC generated noise that can occur
around the filament and hence through the plasma showing up
at the output. (Garscadden, 1986). Powering the filament
with DC voltage eliminated the AC generated noise. The
slightly higher voltage applied to the filament helped
further stabilize the plasma. (Garscadden, 1986). The
length of the tube was 65 cm. This was chosen for optical
gain and vibrational stability. A Jodon model SM-264-2
gain tube with a length of 26 cm and an inside diameter of
2 mm was tried initially because of its size and because it
was on hand. This tube was replaced with a Jodon model

SM-9625-2.5 gain tube 96 cm in length with a 2.5 mm inside diameter because there was not sufficient gain to produce lasing over the length of the perimeter of the ring necessary to accommodate the bias and compensation disks. The 96 cm gain tube was also on hand. It too had to be replaced, but for a different reason. There was more than sufficient gain to produce lasing using this tube, however, due to the length of the tube it could not be supported rigidly enough to stabilize the output. Noise from mechanical and acoustical sources caused the ends of the gain tube to vibrate. This brought about beam competition between the contrapropagating light waves and thus the two beams would not lase simultaneously but alternated back and forth. A Jodon model SM-6512-2.5 gain tube with a length of 65 cm and a 2.5 mm inside diameter was then acquired. It provided both the gain necessary to produce lasing over the desired path length and was also short enough to allow the support required, eliminating the beam competition.

Alignment of the ring laser was achieved with the aid of Lansing model 39.102 VPB 5 mW alignment laser that was transmitted into the ring cavity behind M1 in conjunction with a Hughes model 3025P 5 mW hand held laser that was reflected into the ring cavity between M1 and the Brewster window of the laser gain tube via a beamsplitter assembly. See figure 3.2. For a detailed discussion of the alignment procedures see Appendix B.

Two Ealing model 22-3305 iris diaphragms, I1 and I2,
were positioned halfway between M2 and M3 and halfway
between M1 and M4, respectively. The irises introduced
sufficient losses so that the ring laser cavity would be
operating in the TEM00q axial mode. One of the intracavity
beams was monitored with a spectrum analyzer throughout the
measurements to insure this. The procedure for monitoring
the modes is discussed in Chapter IV.

The beam combiner optics were located behind mirror M3,
the output mirror. It consisted of two mirrors and an OBSC
(output beam splitter cube) fixed to an Al base. See
figure 3.3. The laser beam travelling cw (clockwise)
around the ring cavity entered the OBSC after exiting M3.
The beam travelling ccw (counter clockwise) around the ring
cavity was directed into the OBSC, by the two mirrors,
where it was combined with the cw travelling beam. The
OBSC was mounted onto a goniometer and the two mirrors were
mounted on KS (Klinger Scientific) model PO 46 prism tables
and KS model TR 46 rotation stages to provide enough
adjustment so that the two beams could be aligned
coincident and parallel before entering the detection
system.

The output beat frequency detector circuitry was
furnished by Dr. Hans Bilger, professor at Oklahoma State
University. See figure 3.4. It was designed to convert
the incoming optical signal to approximately 1 volt at 50 Ω

for input to an electronic counter. After exiting the OBSC, the two coincident and parallel contrapropagating beams entered the detection system through a 1 m long optical fiber via a Nippon Sheet Glass model SELFOC OPCL-SG-101 collimator. The optical fiber/collimator was fixed to an NRC model FP-2 fiber positioner mounted directly behind the OBSC. The opposite end of the fiber was coupled to the face of the detector. The detector used was a Silicon Detector model SD100-42-22-231 detector/preamp hybrid type having a GBP (gain bandwidth product) of 20 MHz. The signal from the detector/preamp was amplified by cascading two Burr Brown model 3508J operational amplifiers with a 100 MHz GBP. There was an optical power sensitivity level switch with a 0.1, 1.0, and 10.0 μW range that provided a signal-to-noise ratio of 3.5 dB at 0.1 μW to 28 dB at 100 μW. The output of the beat frequency detector circuit was monitored with an HP model 5335A universal counter, computer controlled for remote operation. The detector and associated circuitry were mounted in an aluminum box for noise suppression. The power supply consisted of two rechargeable 12 volt DC batteries mounted in a separate aluminum box to give 60 Hz isolation.

Drag Site

The optical flats used as the drag and compensation

disks for measurement of the Fresnel drag coefficient were the highest quality of natural fused silica manufactured by Heraeus Amersil identified under the brand name Homosil T-15. The dimensions of the disks were approximately 3" diameter x 2.5" thick. A more accurate measurement of the thickness of the disks will be addressed in Chapter IV. The flats were polished by General Optics to a flatness of $\lambda/20$ with 3 arc seconds parallelism between the two surfaces of each disk.

The Homosil optical flat used for the drag disk was housed in an air bearing mounted to a KS (Klinger Scientific) model SL 20A mirror mount. See figure 3.5. The air bearing was specially manufactured by Dover Engineering. It was floated with zero grade bottled nitrogen at 80 to 100 psi depending on the rotation speed. The nitrogen passed through a 5 μm particle filter before entering the air bearing to reduce any contaminants that might be present. The bearing was rotated using a belt/pulley configuration. See figure 3.6. An Electro-Craft model MT 670 DC motor and model P6300AP DC motor controller were used to drive the air bearing and thus the drag disk. A pulley was mounted to both the outer surface of the air bearing and the shaft of the DC motor. J. P. Coats Dual Duty Plus carpet thread was used as the drive belt. This type of drive belt was chosen because it did not display the stretching or vibration that the rubber

and nylon belts tested had exhibited. This allowed for better speed stabilization and minimum transmission of vibrational noise passed from the motor to the bearing. Rosin was applied to the thread to prevent any slippage through the pulley. The disk was held into the air bearing by rubber O-rings located on each end of the inside diameter of the bearing that were compressed onto the outside circumference of the disk by tightening retainer rings. One of the retainer rings had three nylon screws positioned 120° apart which could be tightened to adjust the parallelism of the disk to the optical axis. This was necessary to reduce, to a minimum, the wobble demonstrated by the disk when the bearing was rotated.

The KS model SL 20A mirror mount provided rotational translation of the disk about both the X and Z axes allowing for both inclination and rotational adjustment. The inclination, or rotation about X, was monitored with an Itek model RI19/35CQPZ(4) optical encoder attached to the hub on the mirror mount for rotation about X. Again, see figure 3.5. The encoder could give rotational position to an accuracy of 2.49 seconds of arc per count. Final adjustment of rotation about both X and Z was performed by adjustment of the micrometers on the SL 20A, accurate to 1.61 arc seconds per division.

The base of the SL 20A mount was attached to X and Z translation stages to control both the horizontal and

vertical position of the disk, respectively. The Z stage

was a KS model MV 120 vertical translation stage that had

an accuracy of 5.0 μm/division. The X stage was a KS model

MT 160 motorized horizontal translation stage that provided

the horizontal displacement Xo of the drag disk. The

accuracy of this stage was 1.0 μm/step. The MT 160 was

driven by a KS model CC-1.2 stepping motor controller that

was interfaced to the computer.

A second KS model MT 160 motorized translation stage

and KS model CC-1.2 motor controller, identical to the one

that provided translation of the optical flat in the X

direction, was used to translate the DC motor along the X

axis as well. This allowed the DC motor to move in

synchronization with the drag disk keeping the drive belt

at a constant tension throughout the measurements. This

was essential for accurate determination of disk position.

Effects of belt tension will be further explained in

Chapter IV.

The rotation rate (f_m) of the drag disk was measured

with a tachometer disk, optical reflector, and an

electronic counter. The tachometer disk was specially

manufactured by Metrilogic with a 7-3/8" outside diameter

and a 4-1/4" inside diameter. It was made of glass and had

two channels of reflective metrifilm lines deposited on the

outer edge. See figure 3.7. This provided for line count

selections of 1200 or 300 both with 50% duty cycles. The

disk was attached to the pulley fixed to the air bearing with the reflective lines facing out. An HP (Hewlett-Packard) model HEDS 1000 optical reflector was mounted above each channel of the tachometer disk on a platform that could be adjusted vertically. In this way the optical reflectors could be focused, optimizing their performance. Either channel could be addressed by computer via reed relays. The output pulses were monitored with an HP model 5335A universal counter that was computer controlled. Before entering the universal counter, the pulses from the optical reflector passed through an adjustable band pass filter to minimize erroneous signals or noise that might add extra counts.

One time base was employed for the HP model 5335A universal counters used to measure the beat frequency (δf_B) and rotation rate (f_m) by connecting the high stability oven oscillator option from one of the counters to the trigger input of both. This insured that the accuracies of the counters were nearly identical and equal to that of the oven oscillator. Comparisons of the two counters were made at various frequencies ranging from 1 KHz to 175 KHz. The highest percentage of variation between the readings on the counters was found to be 0.0003% over the entire frequency range. Any error present in the high stability oven oscillator cancelled out in the calculation of the drag coefficient (α), since both counters operated from the same

time base. See Chapter II equation 2.10.

The compensation disk was inserted into a delrin fixture fastened to a KS model SL 8A mirror mount that was fixed to a KS model MV 120 vertical translation stage for Z axis positioning and KS model MR 120 horizontal translation stage for X axis positioning. This compensated for the beam offset introduced by the drag disk.

Computer Control

The position and rotational speed of the drag disk as well as the data accumulation and processing were automated using a DEC (Digital Equipment Corporation) model LSI 11/2 processor under DEC RT-11 version 5.2 operating system. The software was written in Fortran IV. A National Instruments model GPIBV11-2 IEEE-488 controller was used as the interface between the LSI 11/2 and the Hewlett-Packard counters and Klinger Scientific stepping motor controllers. The rotational speed of the disk was controlled using a Data Translation model DT2781 D/A converter as the interface between the LSI 11/2 and the rotation rate circuitry.
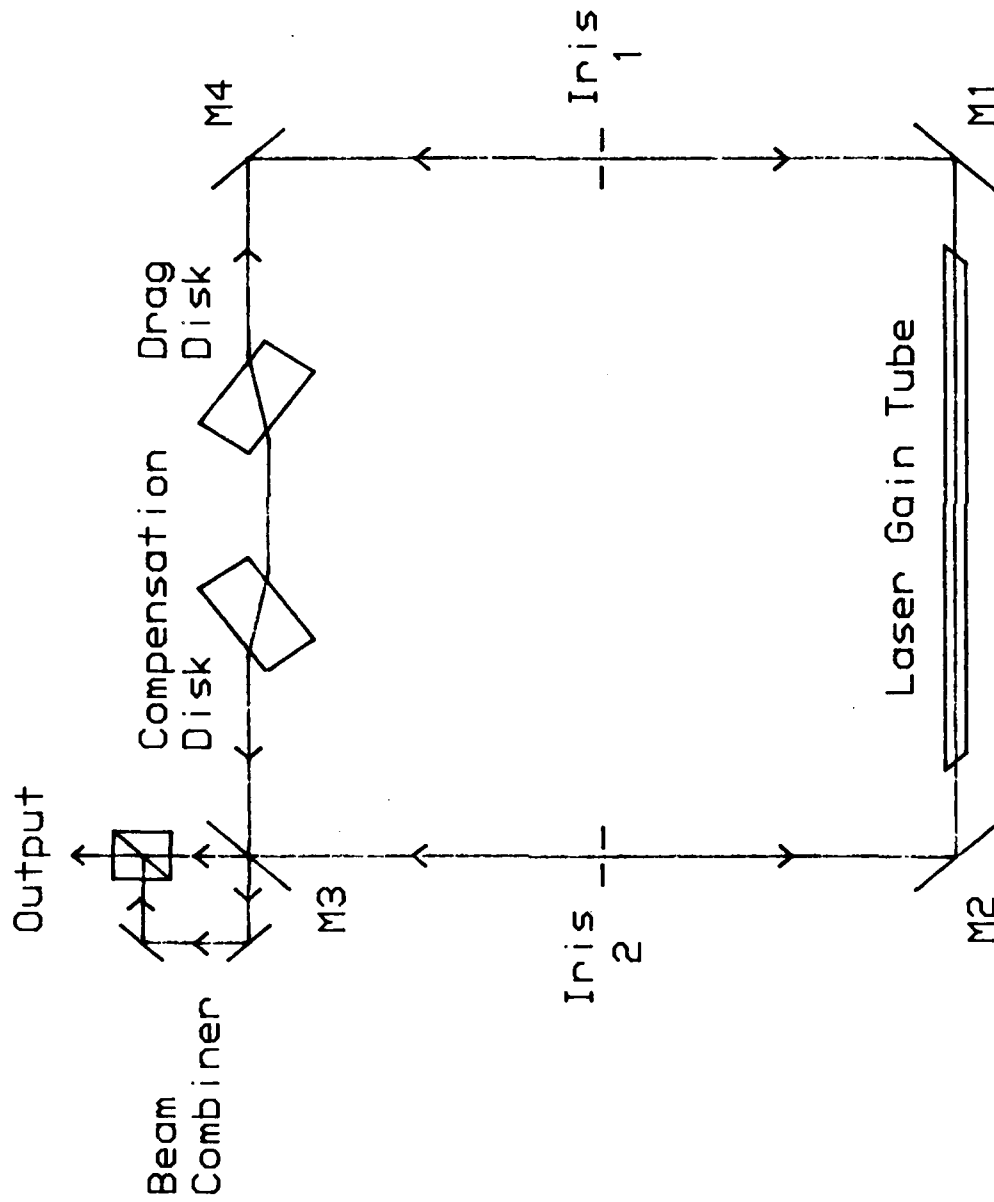
Figure 3.1 - Ring Laser Gyroscope Configuration.

26

- - - - Dashed line signifies position of components and direction of beam when Laser/Beamsplitter Assembly is used.

——— Solid line signifies position of components and direction of beam when Alignment Laser is used.

Laser/Beamsplitter Assembly

Assembly moves in or out of the ring cavity.

Alignment Laser

M1

BS

Laser Gain Tube
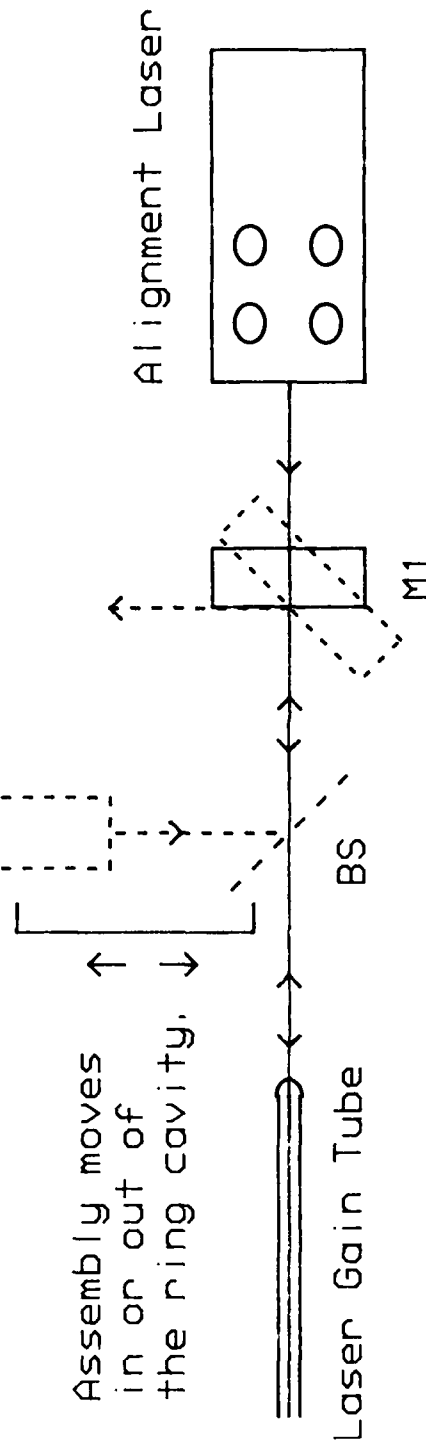
Figure 3.2 - Setup for Ring Cavity Alignment.
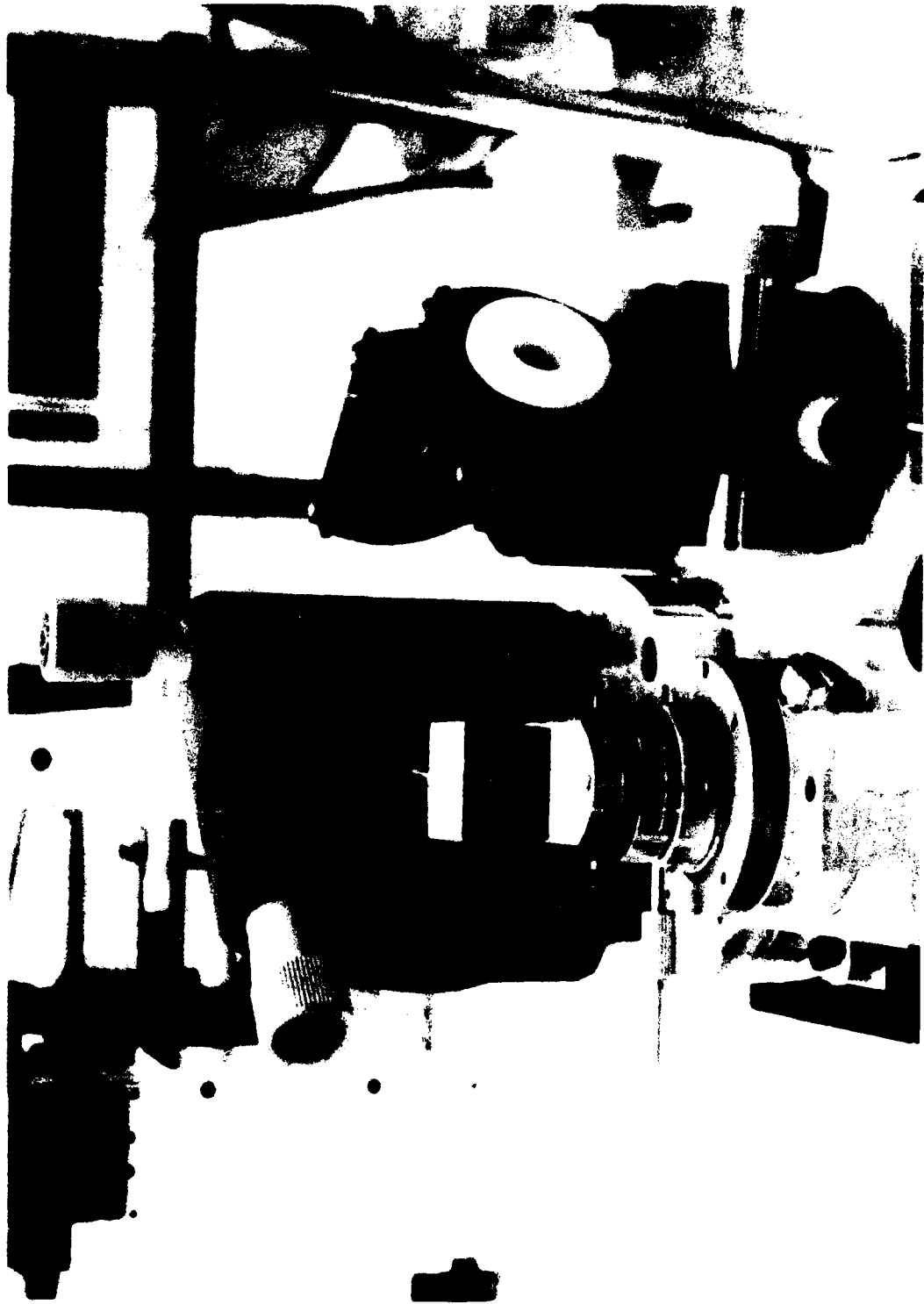
Figure 3.3 - Beam Combiner Optics.

All resistances in ohms.

All capacitance in micro-
farads unless stated
otherwise.

U1 = SD100-42-22-231

U2 = U3 = BB 3508J

Ring Laser
Output
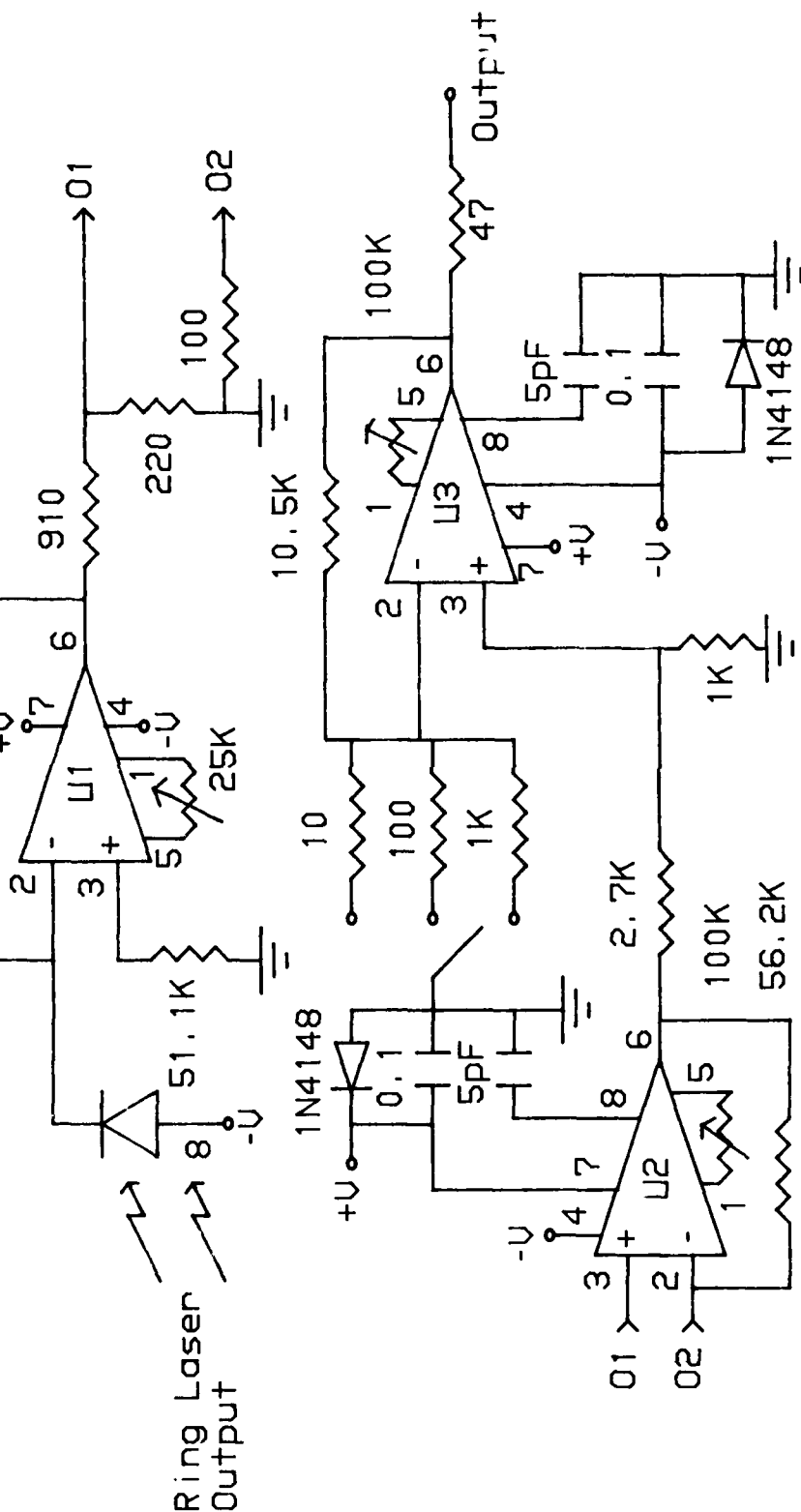
Figure 3.4 - Beat Frequency Detector Circuit.

Figure 3.5 - Drag Disk Mount.
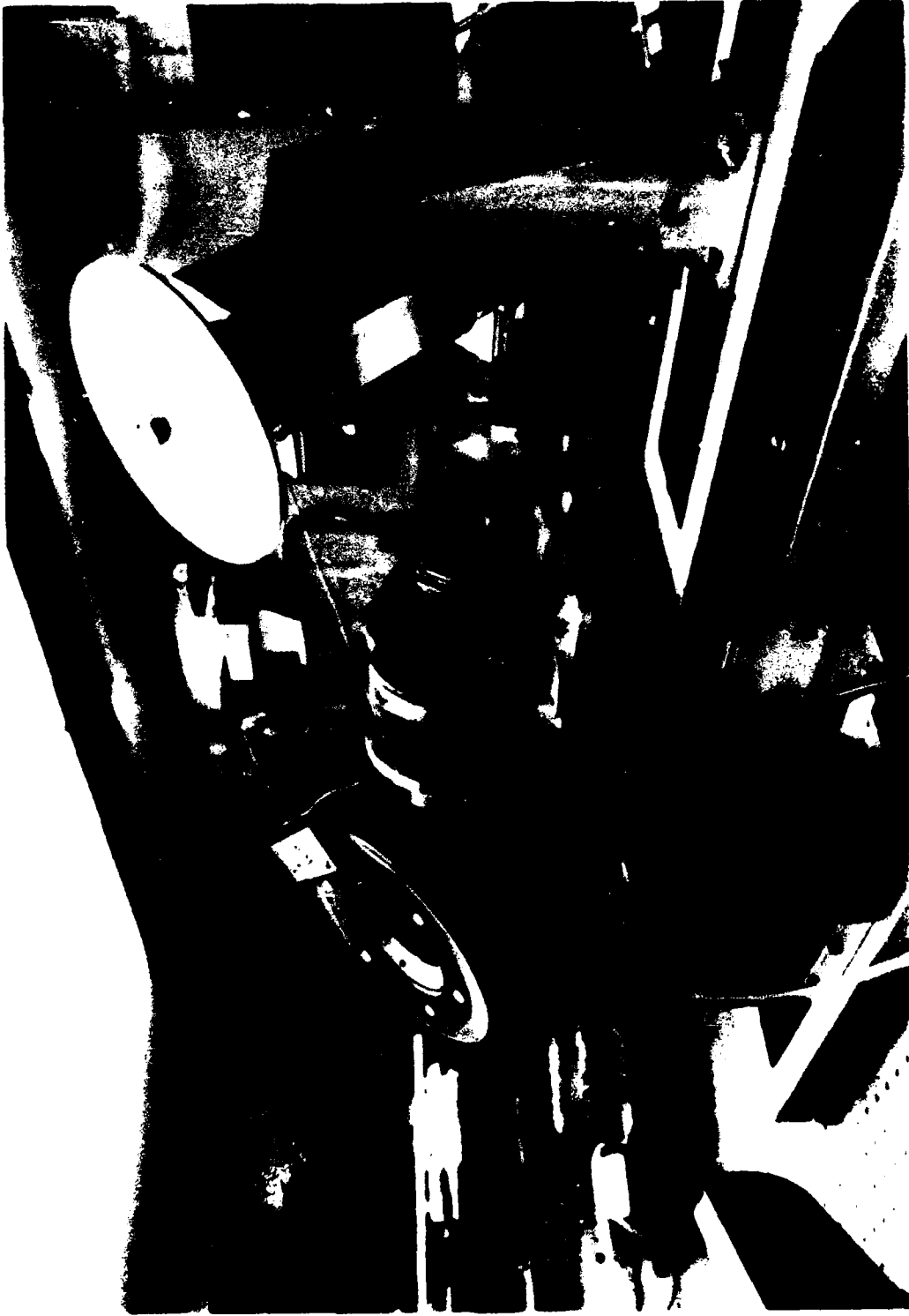
Figure 3.6 - Drag Disk Rotation Setup.
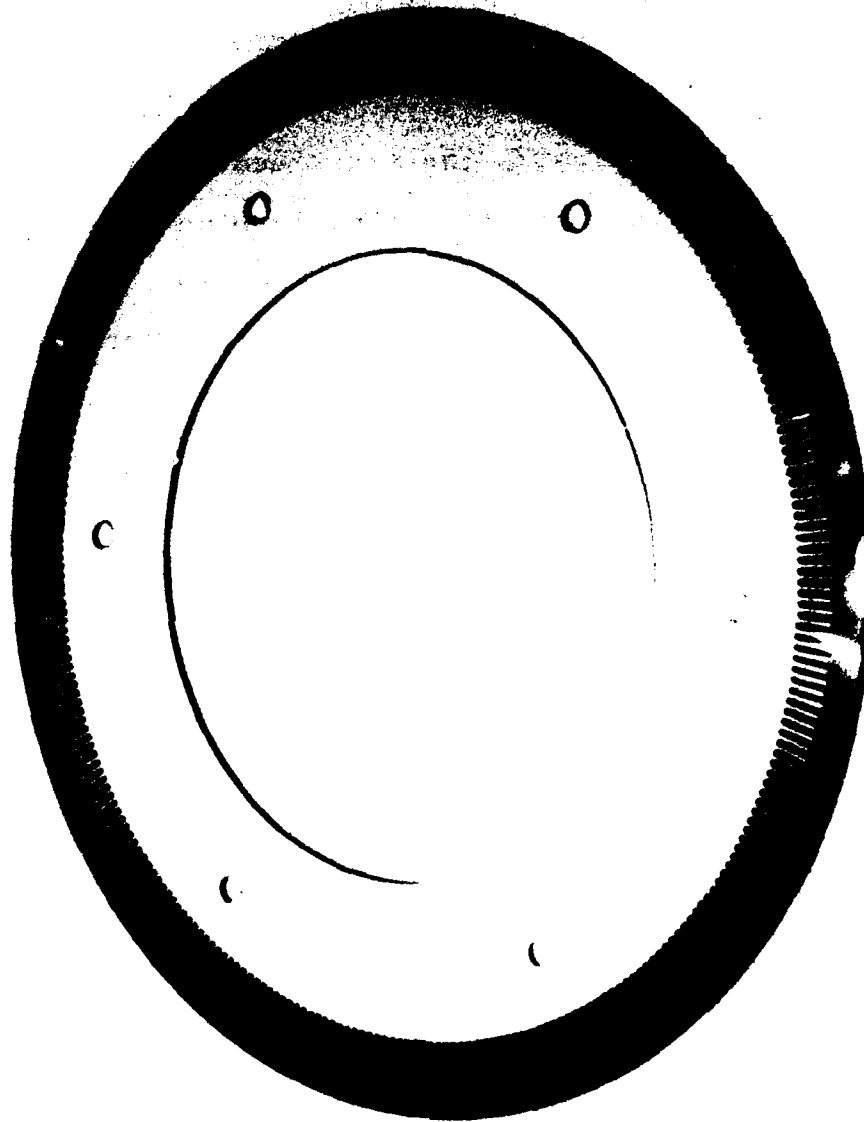
Figure 3.7 - Tachometer Disk.

CHAPTER IV

EXPERIMENTAL PROCEDURES

This chapter covers the experimental procedures used to measure the parameters for determination of the drag coefficient α along with the accuracy in which these parameters could be measured. This includes the preparation of both the drag disk and compensation disk. The order of the procedures presented here is the order in which they were carried out during this experiment. All recorded data for the calculation of α is given in the following chapter.

Wavelength (λ)

The value of the wavelength for a HeNe laser in air, the case employed for this experiment, was taken from a table of laser lines. (Striganov-Sventitskii, 1968). λ was given to an absolute accuracy of $\pm$ 4 x 10^{-15} m.

Drag Disk Thickness (1)

The thickness of the drag disk was measured with a J&L (Jones and Lamson) model VIVIC automatic gaging system connected to a Bausch and Lomb model ACURITE II digital

32

position readout. The system provided a non-contact measurement that was calibrated to an accuracy of $\pm$ 0.000102" using a J&L model 901 certified calibration standard. The thickness was measured 7 times, rotating the disk after each measurement by 90° about the axis parallel to the scan direction. The data was then converted to metric and averaged. This measurement was performed with an absolute accuracy of $\pm$ 3.6 μm. The effects of thermal expansion were considered and found to be significantly less than the accuracy with which the measurement could taken. The average coefficient of thermal expansion for natural fused quartz at 273°K to 373°K is $5.1 \times 10^{-7}/^{\circ}$K. (Heraeus Amersil, 1981). A variation of $\pm$ 10°C about room temperature would change the thickness of the disk by $\pm$ 0.3 μm.

Refractive Index (n) and Dispersion (dn/dλ)

The equipment required to measure, directly, the refractive index and dispersion of the drag disk was not available. Therefore, n(λ) and dn/dλ were determined mathematically using a dispersion formula given by Rodney and Spindler. (Rodney-Spindler, 1954). A five point interpolation of n(λ = 632.81646 nm), based on Aitken's method, was calculated from the data given by Rodney-Spindler for n(λ) about n(λ = 632.81646 nm) at T = 24°C. This was performed for comparison to the value n(λ)

calculated from the dispersion equation. Error in the values of $n(\lambda)$ used to determine $n(\lambda = 632.81646$ nm$)$ do not exceed $\pm 1 \times 10^{-5}$.[1] (Rodney-Spindler, 1954).

Preparation of the Drag and Compensation Disk

The lock-in frequency of a ring laser gyro increases with scatter (Killpatrick, 1967), therefore it was imperative to get both the drag and compensation disk as clean as possible. The cleaning procedures outlined below were executed on each side of both the drag disk and the compensation disk with cleaning of the drag disk performed last.

Visible particles, such as dust and lint, were first removed from the surface of the disk with Texwipe Micro Duster compressed air that was passed through a 0.0012 mm pore size filter. One end of a lens cleaning tissue, 3 times the diameter of the disk long and 1.5 times the diameter of the disk wide, was placed across the surface so as to cover the entire surface. The 1/3 portion of the tissue covering the disk was wetted with Baker spectrophotometric grade acetone until the surface of the disk was completely saturated. The remaining 2/3 was dragged across the surface until all the acetone was

---

[1] The temperature dependence of n for natural fused quartz is $1.01 \times 10^{-5}/^{\circ}C$ at $\lambda = 632.8$ nm and $T = 30^{\circ}C$. (Rodney-Spindler, 1954).

removed. The spectrophotometric grade of acetone was analyzed to leave a maximum of 0.00005% of residue after evaporation. This cleansing was performed several times. The process was then repeated dragging the lens cleaning tissue across the surface 90° to the direction it had been dragged previously. This was also performed several times. The solvent was then changed to Baker spectrophotometric grade methanol and the surface dragged in the same manner as had been carried out using acetone. The spectrophotometric grade methanol was analyzed to leave a maximum residue of 0.0002% after evaporation. A few final drags were performed using acetone due to the fact that it left the least amount of residue after evaporation. Next, the surface of the disk was covered with a thin coat of Matheson, Coleman and Bell non-plasticized collodion to remove any remaining residue. The collodion was allowed to become rubbery in texture, dry but not brittle, and peeled off with a pair of tweezers clamping onto one edge of the collodion pulling it up and over the surface as one would remove a piece of tape. A small, low wattage, hand held, HeNe laser was used to illuminated the surface to look for scatter centers from remaining residue. This process was repeated until no scatter centers could be observed by the eye with the laser. This assured the cleanliest, lowest scatter surface possible.

The order in which the solvents were used, acetone-

methanol-acetone, for dragging the surface of the disk was
arrived at through trial and error. It was found that by
following the process outlined above, the fewest number of
coats of collodion were needed to remove the remaining
residue. The number of coats of collodion applied averaged
8 for the above process whereas, for other processes tried,
the average number of coats rose to 12.

Setting the Normal Angle

The normal angle of the drag and compensation disk was
determined using a Kollmorgan model K-222 dual axis
autocollimator positioned directly behind mirror M2 facing
in the direction of M3. See figure 4.1. By lookirg
through the eyepiece of the autocollimator, and hence
through the backside of M2, one could observe the
intracavity laser beam. Goggles providing attenuation were
utilized to reduce the beam power sufficiently to allow
this direct viewing. With both disks removed, the
autocollimator was aligned to the intracavity beam by
positioning the autocollimator so that the center of the
beam was matched to the intersection of the fixed
horizontal and vertical crosshairs seen through the
eyepiece of the autocollimator. This was performed by
translating the movable horizontal and vertical crosshairs,
also seen through the eyepiece of the autocollimator, back
and forth on either side of the fixed crosshairs out to the

edge of the beam, adjusting the position of the
autocollimator until the movable crosshairs translated an
equal distance in both directions from the fixed
crosshairs. The movable crosshairs were attached to a
vernier with a readout of 0.10 arc seconds/division. The
procedure for aligning the autocollimator could be repeated
to within $\pm$ 1 arc second. Next, the drag disk was inserted
into its mount and aligned normal to the laser cavity so
that lasing occurred. The transmitted portion of the
intracavity beam through the disk, as well as the reflected
portion from the disk surface, could be observed with the
autocollimator. The micrometer providing rotation about
the Z axis on the KS (Klinger Scientific) model SL 20A
mount housing the drag disk was positioned so that the
reflected beam was above or below the transmitted beam.
This was done to aid in alignment. The reflected beam was
aligned to the fixed vertical crosshair in the same manner
as had been done to align the autocollimator. However,
instead of adjusting the autocollimator, the micrometer
providing rotation about the Z axis on the KS model SL 20A
was translated until the movable vertical crosshair
traveled an equal distance in both directions from the
fixed vertical crosshair out to the edge of the reflected
beam. The position of the micrometer was recorded and then
translated to move the reflected beam to either the left or
the right of the transmitted beam in order to adjust the

reflected beam to the fixed horizontal crosshair. The
micrometer for rotation about the X axis on the KS model SL
20A was then adjusted in conjunction with the horizontal
movable crosshair on the autocollimator until alignment
with the horizontal fixed crosshair was achieved in the
same way as had been done to position the reflected beam
with the vertical crosshair. The micrometer on the KS
model SL 20A providing rotation about Z was then moved back
to the recorded location, positioning the reflected beam
directly on top of the transmitted beam. The procedure for
alignment of the reflected beam to the transmitted beam
could be repeated with an accuracy of $\pm$ 1 arc second. The
compensation disk was then inserted into its mount and the
same process was followed for that disk as had been
performed for the drag disk. This also had a repeatability
$\pm$ 1 arc second. Both drag and compensation disk were now
at normal angle to the intracavity beam within $\pm$ 1 arc
second.

Drag Disk Wobble

Wobbling of the drag disk when it rotated caused the
reflected beam to drift off center. This observation was
made through the autocollimator. The calibrated scales,
seen through the eyepiece of the autocollimator, provided a
way to measure the amount of drift of the reflected beam.
The wobble could be minimized by adjustment of the three

nylon screws on the retainer ring holding the drag disk in place. See Chapter III. The disk was spun after each adjustment to check the amount of wobble with the autocollimator. Using this method it was possible to reduce the drift of the reflected beam to $\pm$ 2.5 arc seconds in any direction off center.

After the wobble had been minimized, the normal angle was again verified, following the procedures above, to insure that the disk was still normal to the intracavity beam.

Inclination Angle (β) of the Drag Disk

The inclination angle (β) at which the drag disk was positioned for this experiment was set by observing the readout of an AI (angle indicator) for the Itek model RI19/35CQPZ(4) optical encoder as the optical flat was rotated about the X axis. The disk was rotated clockwise, as one would observe standing between mirrors M3 and M4, outside the ring cavity, looking in towards the center of the ring, until the AI reading was approximately 48°. The accuracy of the optical encoder was $\pm$ 2.49 arc seconds. Final adjustment of β was made using the micrometer for rotation about the X axis on the KS model SL 20A mount housing the drag disk. This micrometer had an accuracy of 1.61 arc seconds/division or 3.22 divisions/reading change on the AI display. By translating the micrometer until the

readout just changed, always translating in one direction never translating back, the angle which appeared on the AI display was accurate to $\pm$ 1.61 arc seconds. When this was accomplished, the compensation disk was rotated in its mount about the X axis counter clockwise, using the same reference frame as above, until lasing occurred. Observation was made through the autocollimator to assure that the intracavity beam was still positioned at the intersection of the fixed horizontal and vertical crosshairs. The micrometer for rotation of the compensation disk about the X axis was adjusted until the center of the beam and the intersection of the crosshairs did indeed match, using the same procedures that were used to set the normal angle.

The inclination angle was not set to Brewster angle as had been done in the two preceding experiments. With the disk at Brewster angle, the intracavity beam was very close to the edge of the polished surface on both sides of the disk. This was because of the thickness of the optical flat used. See figure 2.2, Chapter II. After the disk was in place in the mount, it was observed that the outer edge of the polished surface of the disk was not as clean as the portion of the surface closer towards the center. This was due to handling the disk during insertion into the mount. It was also observed that as the disk rotated, the outer edge of the surface accumulated dust more readily than did

the region of the surface towards the center. It is believed that this might have been due to the gas exiting from the air bearing, setting up air currents at the surface of the disk. A hood was installed that slowed down the dust accumulation, but did not eliminate it. See figure 4.2. In addition, prior to rotation of the disk, the surface of the drag disk was blown with deionized nitrogen using a static eliminator gun to reduce the static attraction of dust particles. This further reduced the rate in which dust accumulated, however, it did not eliminate the dust problem completely. Therefore, to operate the experiment on the cleanliest region of the surface of the drag disk possible, β was set to the minimum angle that would allow enough gain for lasing and provide for the intracavity beam to be located closer to the center portion of the surface of the disk.

Center of Rotation of the Drag Disk

The autocollimator was implemented to locate the center of rotation of the optical flat. After the disk was positioned at the intended inclination angle it was set into a rotation of 90 rpm. This was performed with the computer that controlled several pieces of equipment and recorded three of the parameters. See "Beat Frequency and Drag Disk Rotation Rate and Position" below. With the KS (Klinger Scientific) model CC-1.2 stepper motor controller

for translating the drag disk along the X axis in the local mode, the disk was positioned so that the intracavity laser beam was near the edge of the face of the disk. Looking through the autocollimator, the disk was translated towards the edge in single steps until the beam was finally extinguished. The position on the motor controller was recorded. The disk was then translated in the opposite direction until the beam was again visible and the process repeated. This was done several times for error analysis. The same process was then performed on the opposite edge of the face of the disk. The center of rotation was determined by halving the difference between the two positions for the edge location. When locating the position of the edge of the flat, it was imperative that the tension of the disk drive belt was the same at each edge. Therefore, the tension was measured with a Waters Manufacturing model 651C1 torque watch gage with a hook attached to a string wrapped around a post inserted into the chuck of the torque gage. The hook was positioned in the center and under the drive belt. A ruler was placed vertically behind the belt to read the change in vertical position of the belt. The drive belt was then pulled up by the torque gage, reading the tension for a 1" vertical change in the belt position. If the torque reading on the one side of the disk was different than that on the other side, the tension could be adjusted by positioning the DC

drive motor. This was accomplished by translating the KS
model CC-1.2 stepper motor controller for the stepper motor
that moved the DC motor along the X axis.

Measurement of the belt tension was necessary because
it was found that the more tension there was in the belt,
the further the position of edge of the disk, and thus the
center of rotation, would shift in towards the DC motor
driving the disk. The tension of the belt would change
with position of the disk because of the fact that the disk
was on the vibration isolation table and the DC drive motor
was not. The weight of the motor shifted on the table as
it was translated and the table would then shift to
compensate for the redistribution of the weight. This in
turn would change the belt tension since the drive motor
did not change its position. Taking the tension of the
belt into consideration, the accuracy with which the center
of rotation could be determined was $\pm$ 4 μm. For analysis
of the shift in the center of rotation due to belt tension,
see Appendix C.

Optical Path Length (L)

The optical path length (L) of the ring laser cavity
was measured with both the drag disk and compensation disk
in the cavity and at the intended inclination angle.
Measurement of L was performed by observing the beat
frequency between three axial modes where the beat

frequency is given by

$$\delta f_L(k) = kc/L \qquad\qquad 4.1$$

where δf_L is the beat frequency between two axial modes, k
= 1 for the beat frequency between axial modes one and two
and k = 2 for the beat frequency between axial modes two
and three, c is the speed of light in a vacuum and L is the
optical path length of the ring laser cavity.

Inclusion of three axial modes was done to provide
higher accuracy, giving a mean value of

$$avg(\delta f_L) = (1/2)\sum_{k=1}^{2}(\delta f_L(k)/k). \qquad\qquad 4.2$$

The irises between M2-M3 and M1-M4 were opened all the
way to allow as many modes as possible to be present in the
intracavity beam. The beat frequencies between the various
modes were observed using the portion of the intracavity
beam that was reflected upwards from the surface of the
compensation flat. The beam was directed onto a modified
TI (Texas Instruments) model TIX55 photo diode and the
signal then amplified in stages using an HP (Hewlett-
Packard) model 8447A preamplifier and an HP model 8447F
amplifier. The output from the HP 8447F was displayed with
an HP model 8555A spectrum analyzer section installed into
an HP model 141T display unit. Also inputted to the

spectrum analyzer was an HP model 8640B-OPT.323 signal
generator that was displayed simultaneously along with the
beat frequencies. The output frequency from the signal
generator was also measured with an HP model 5335A
universal counter. See figure 4.3.

The spectrum analyzer was first adjusted to display
$\delta f_L(1)$. Next, the frequency of the signal generator was
adjusted until it was observed directly on top of $\delta f_L(1)$ so
that only one peak could be seen. The counter readout was
recorded. This was performed 30 times for error analysis.
The spectrum analyzer was then adjusted to display $\delta f_L(2)$
and the process was repeated. These quantities were used
in equation 4.2 to calculate $avg(\delta f_L)$ which was substituted
into equation 4.1 for δf_L from which the optical path
length was determined. The accuracy with which the optical
path length could be measured was within $\pm$ 260 μm.

Beat Frequency and Drag Disk Rotation Rate and Displacement

The remaining parameters, δf_B, f_m and Xo, were measured
via a DEC (Digital Equipment Corporation) model LSI 11/2
computer. See Chapter III. In addition to recording the
measurements, the computer also controlled the position and
rotation rate of the drag disk. The computer would send
signals through an IEEE 488 interface, controlling the
displacement of the optical flat from the center of
rotation. A Data Translation model DT2781 D/A converter,

connected to the DEC processor through the backplane, would

output a particular voltage to the Electro-Craft model

P6300AP DC motor controller that corresponded to a

particular speed. The output from the tachometer

circuitry, giving the rotational speed of the disk,

provided feedback to help maintain the disk speed to within

0.06%.

The computer first positioned the drag disk to an

arbitrary, but known, Xo. The drive belt tension was

adjusted to the same tension as it had been set for

location of the center of rotation of the disk, following

the procedures outlined in that section above. The disk

was then rotated at an arbitrary rotation rate and the

irises between M2-M3 and M1-M4, respectively, were closed

down until only the TEM00q mode was visible on the display

for the spectrum analyzer. The beat frequency signal was

observed and the filters adjusted until a low noise signal

was present on the oscilloscope display and hence, measured

by the counter. The computer then rotated the disk from

near 0 rpm to 900 rpm in both the clockwise and counter

clockwise directions in increments of 100 rpm per set of

beat frequency/rotation rate measurements. Ten readings

over a 10 second period were taken at each rotation rate

for error statistics. Next, the computer rotated the disk

at an arbitrary, but known, rotation rate and positioned

the disk at -10 mm to +10 mm with respect to the center of

rotation, in increments of 1 mm, stopping disk rotation before each set of measurements to allow belt tension adjustment. Again, ten readings over a 10 second period were recorded. The data was finally processed and curves plotted of δf_B versus f_m and Xo.

Figure 4.1 - Autocollimator Position.

Figure 4.2 - Drag Disk Hood.
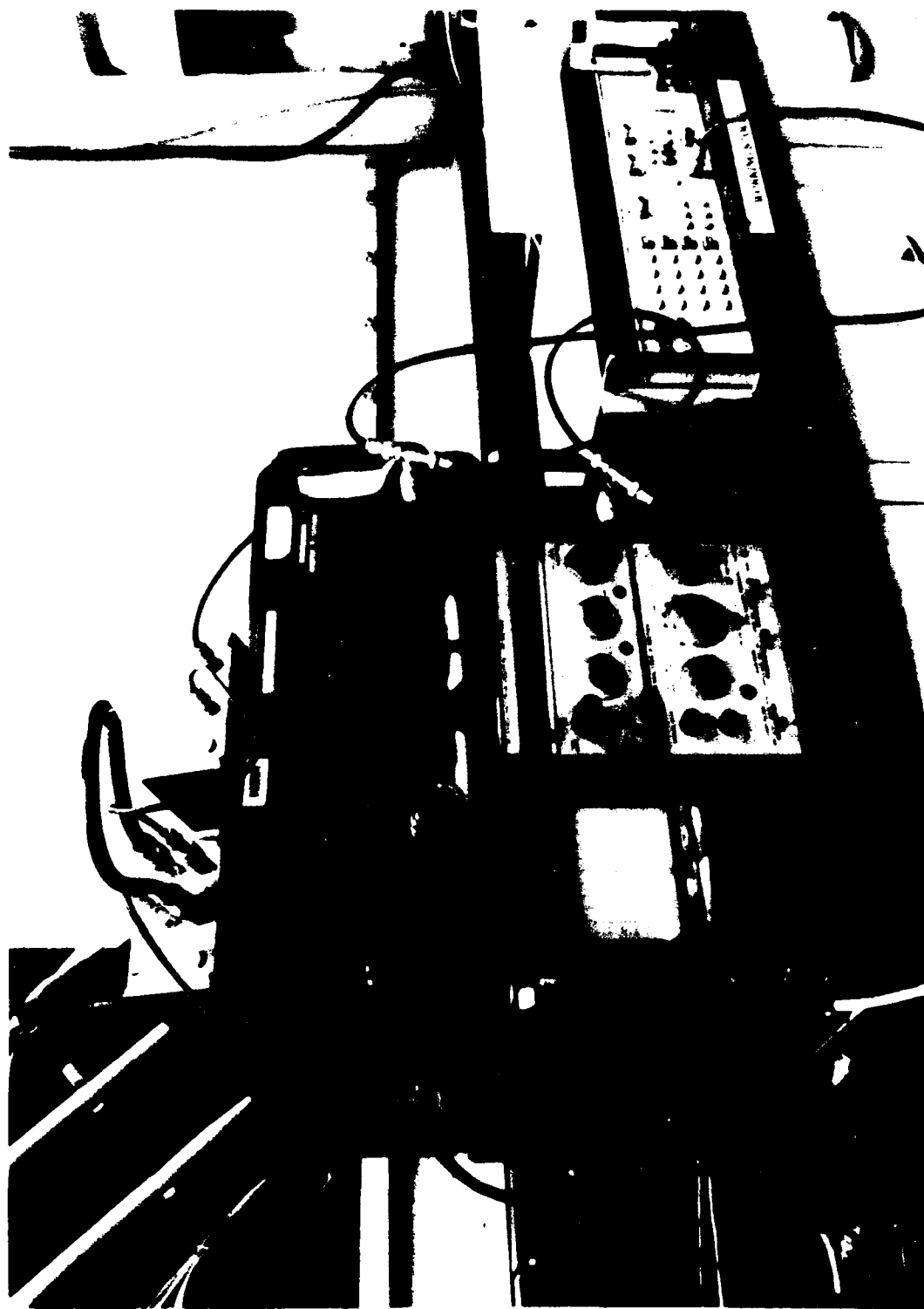
Figure 4.3 - Measurement Equipment to Determine Optical Path Length.

CHAPTER V

RECORDED DATA AND OBSERVATIONS

The data presented in this chapter is a collection of all of the parameters that were used to calculate the Fresnel drag coefficient (α), following the procedures outlined in the preceding chapter. The data that remained fixed is presented in table 5.1 in the order measured or calculated.

TABLE 5.1
MEASURED PARAMETERS (CONSTANT)

Parameter	Nomenclature	Quantity	Error ($\pm$ %)
λ	Wavelength (in air)	0.63281646 μm	0.0000008
l	Drag Disk Thickness	61.124 mm	0.006
n	Refractive Index	1.45707	0.0007
$dn/d\lambda$	Dispersion	-0.0290785 $(\mu\text{m})^{-1}$	0.0007
β	Inclination Angle	47.9855°	0.0009
L	Optical Path Length	4.2447 m	0.006
Xo^1	Displacement	8.000 mm	0.05
δf_{Bs}	Beat Frequency due to Sagnac Effect	78.3 Hz	0.17

[1] The belt tension was 0.1 oz. for the measurement of Xo.

Table 5.2 is a presentation of the experimentally determined beat frequency (δf_B(exp.)) versus the rotation rate (f_m). A positive rotation rate is defined as clockwise, viewed from mirror M4 towards M3.

TABLE 5.2
BEAT FREQUENCY VERSUS ROTATION RATE

f_m (rpm)	Error (± Percent)	δf_B(exp.) (Hz)	Error (± Percent)
-881.22	0.07	-26524.5	1.67
-823.95	0.08	-23559.4	1.61
-713.65	0.03	-17934.8	1.93
-608.20	0.02	-15397.1	0.41
-507.52	0.02	-12888.1	0.46
-405.08	0.01	-10423.6	1.03
-299.94	0.01	- 7975.2	0.56
-195.22	0.02	- 5735.0	0.86
-101.22	0.02	- 4133.7	2.16
0.23	45.36	1805.3	55.82
96.76	0.02	4252.1	3.85
203.18	0.03	6112.0	1.48
299.16	0.03	8270.3	1.63
396.32	0.01	10533.4	0.96
500.80	0.09	13063.0	0.43
595.56	0.04	15250.8	0.82
686.73	0.03	17415.2	0.65
783.67	0.09	21875.6	1.07
877.47	0.07	25439.5	0.35

Table 5.3 is the recorded data of beat frequency versus the displacement of the drag disk from the center of rotation. A positive displacement is defined as the right hand side of the disk, viewed from mirror M4 towards M3.

Throughout the duration of these measurements, the display for the spectrum analyzer was observed to assure

TABLE 5.3
BEAT FREQUENCY VERSUS DISPLACEMENT

f_m (Hz)	Error ($\pm$ Percent)	Xo[1] (mm)	δf_B(exp.) (Hz)	Error ($\pm$ Percent)
497.56	0.02	−10.000	−16121.4	0.26
497.76	0.04	− 9.000	−14583.0	0.17
497.72	0.03	− 8.000	−12979.4	0.37
497.95	0.06	− 7.000	−11432.4	0.47
497.86	0.03	− 6.000	−10060.5	0.93
497.89	0.04	− 5.000	− 8633.2	0.56
497.75	0.04	− 4.000	− 7247.5	0.87
497.92	0.03	− 3.000	− 6088.0	0.88
497.81	0.04	− 2.000	− 4917.6	1.30
497.72	0.03	− 1.000	− 4509.7	7.21
497.88	0.02	1.000	4395.5	1.88
498.04	0.04	2.000	4811.2	1.62
498.08	0.02	3.000	5893.6	1.76
498.13	0.04	4.000	7233.6	0.78
498.08	0.04	5.000	8697.7	1.10
498.24	0.04	6.000	10086.8	0.67
498.25	0.03	7.000	11491.1	0.79
498.33	0.03	8.000	13038.1	0.88
498.48	0.02	9.000	14521.7	1.19
498.68	0.06	10.000	16102.9	0.45

that only the TEM00q mode was present. Also observed was the oscilloscope display of the beat frequency after filtering to gauge the amount of noise that was getting through to the counter. For most of the measurements the signal appeared clean, a low noise signal. See figure 5.1. For some of the measurements, particularly the ones taken for the rotation rates −100 rpm $\leq$ f_m $\leq$ 100 rpm, noise

[1] The measurement of Xo had an absolute error of $\pm$ 4 μm for a belt tension of 0.1 oz.

could be observed with the signal. The filtering circuit could not filter the noise without significant attenuation of the beat frequency signal. The counter then could not detect the attenuated signal.
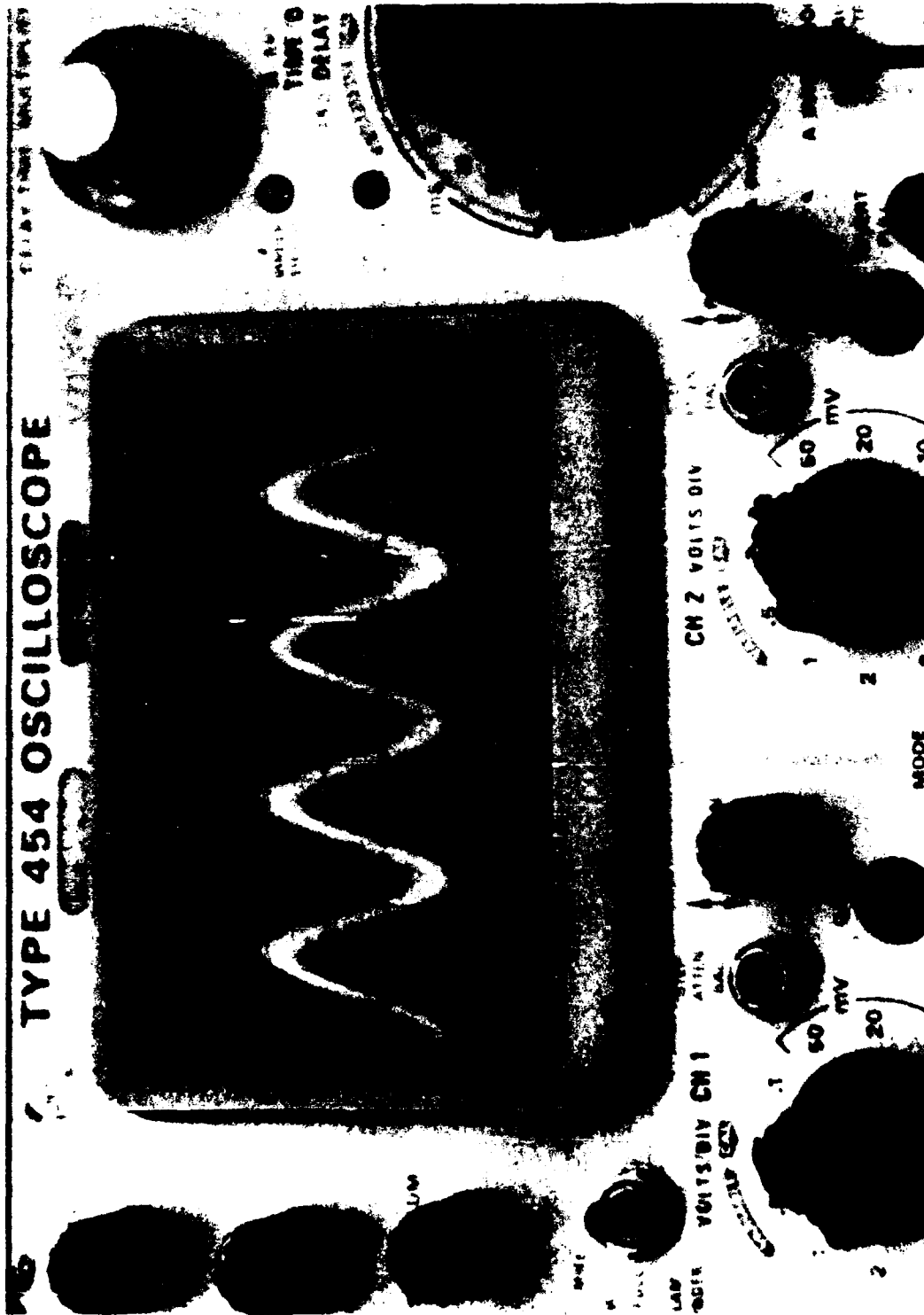
Figure 5.1 – Beat Frequency Signal.

CHAPTER VI

RESULTS

The graphical representations of tables 5.2 and 5.3,
Chapter V, are shown in figures 6.1 and 6.2, respectively.
The Fresnel drag coefficient (α) was determined from this
experimental data and compared with α_{Lo}, which was
calculated from the Lorentz equation 2.2 in chapter II, and
α_{La}, which was calculated from the Laub equation 2.5 in

TABLE 6.1
FRESNEL DRAG COEFFICIENTS

Symbol for Coefficient	Value of Coefficient	Error ($\pm$ Percent)
avg α_{fm}[1]	0.352	2.8
avg α_{Xo}[2]	0.360	3.3
avg α_{exp}	0.356	4.3
α_{Lo}	0.541609	0.0007
α_{La}	0.537648	0.0007

[1] Fresnel drag coefficient determined by using the data
from Table 5.2 where Xo was constant and f_m was varied.

[2] Fresnel drag coefficient determined by using the data
from Table 5.3 where f_m was constant and Xo was varied.

Chapter II. See table 6.1. The values for the refractive index of the disk, dispersion of the disk and wavelength of the light in air were taken from table 5.1, Chapter V, and used in both equations 2.2 and 2.5. To determine avg α_{fm} and avg α_{Xo} from the experimental data, the average of only those points on the linear portions of both curves were used. The value of avg α_{exp} is the average of all the data points employed to determine avg α_{fm} and avg α_{Xo}.

Table 6.2 compares the accuracy of the experimental value of the Fresnel drag coefficient determined in this experiment (avg α_{exp}) to the accuracy of the experimental value of the Fresnel drag coefficient determined in the Bilger-Stowell experiment (α_{BS}). As can be seen, the

TABLE 6.2
avg α_{exp} VERSUS α_{BS} (ACCURACY)

%error avg α_{exp}	4.30 %
%error α_{BS}	0.07 %

accuracy with which the drag coefficient could be determined is far better in the previous experiment. Table 6.3 compares the experimental and theoretical values of the Fresnel coefficient for both this experiment and the Bilger-Stowell experiment. The differences between the experimental and theoretical values, as can be seen in Tables 6.1 and 6.3 are quite significant. Possible reasons

TABLE 6.3
avg α_{exp} VERSUS α_{theor}

avg α_{exp}/α_{Lo}	65.70 %
avg α_{exp}/α_{La}	66.20 %
α_{BS}/α_{Lo}	0.17 %
α_{BS}/α_{La}	0.91 %

for these differences as well as the poor accuracy are covered in the next section.

Evaluation

Several explanations for the difference between α_{exp} and α_{theor} were explored. It is believed that the measurement of the beat frequency was the most probable source of error. First of all, measurement of δf_B was the least accurate of all of the parameters. Several schemes to improve the accuracy and reduce the noise were tried. 3/4" diameter glass tubes were inserted into the ring cavity between all mounts so as to encase the intracavity laser beams. See figure 4.1 in Chapter IV. This was done to determine if any cross currents of air were contributing to the noise in the beat frequency signal. Noise present in the beat frequency before insertion of the glass tubes, observable on the oscilloscope, was reduced after insertion. However, this did not alter the beat frequency

as measured by the counter. The glass tubes were in place for the data recorded in Chapter V.

The beat frequency detector electronics were inspected and it was found that there were several unattached wires on the circuit board. This detector circuit was removed and a United Detector Technology model PIN 10 photodetector and model 101B amplifier were substituted with the same results. This verified the performance of the beat frequency detector eliminating it as a possible contributor of error.

Noise caused a problem to accurately measure the beat frequency signal over the entire range. Therefore, processing of the beat frequency signal was experimented with by varying the passband of the filter. This had quite a dramatic effect on what the counter measured. One could effectively dial in whatever frequency one desired, regardless of the actual frequency. Because of this, the filter was set so that the frequency of the signal measured by the counter was the same as the frequency observed on the oscilloscope. This was performed prior to the measurements with a disk rotation speed of 100 rpm. It was not readjusted for the remainder of the measurements. In retrospect, the pass band of the filter should have been optimized for each beat frequency measurement. Also, the bandwidth of the filter should have been much narrower. This will be covered in the next chapter.

It was suggested, after the experiment was completed, that the optical encoder and angle indicator did not record the correct inclination angle and that the angle was actually close to Brewster angle. This would indeed render experimental results which would more closely correspond with theory. However, not being present to actually observe this, the suggestion surmised cannot be taken as seriously as one would desire. Even at Brewster angle, using all remaining parameters as recorded, the experimental value of α would still be 14% less than the theoretical value. Also, the repeatability with which the angle was measured throughout the experiment makes this explanation less viable.

Due to the extreme thickness of the drag disk, the manufacturer could only provide a best effort attempt at polishing the disk, resulting in 3 arc seconds parallelism between the surfaces of the disk. This, in conjunction with the size of the perimeter of the ring cavity, prevented the elimination of wobble. The intracavity beams wandered and the intensity of the beams periodically diminished as the disk rotated. The beat frequency was thus being modulated by the wobble. Observation on the oscilloscope revealed that the amplitude of the beat frequency was between 0.5 and 1.0 volts peak-to-peak for approximately 2/3 of a revolution of the drag disk and near zero for approximately 1/3 of a revolution of the disk.

Hence, the signal could not be measured for 1/3 of the time due to the fact that the amplitude of the signal, throughout that 1/3 of a revolution of the disk, was too low for the counter to read. The computer program for this experiment configured the counter, set in the remote mode, to continuously take measurements over a ten second interval and then average them to get the final value of the beat frequency. The filter adjustment prior to recording the data was, therefore, not performed correctly as it was later realized that this was done with the counter in the manual mode. This set the counter to take readings at a different measurement rate and over a different time interval than for the computer controlled remote mode. It is conjectured that this largely accounts for the difference between the experimental and theoretical values of α as well as the accuracy differences between this experiment and the Bilger-Stowell experiment. This could not be proven, however, because it was discovered after the conclusion of the experiment.
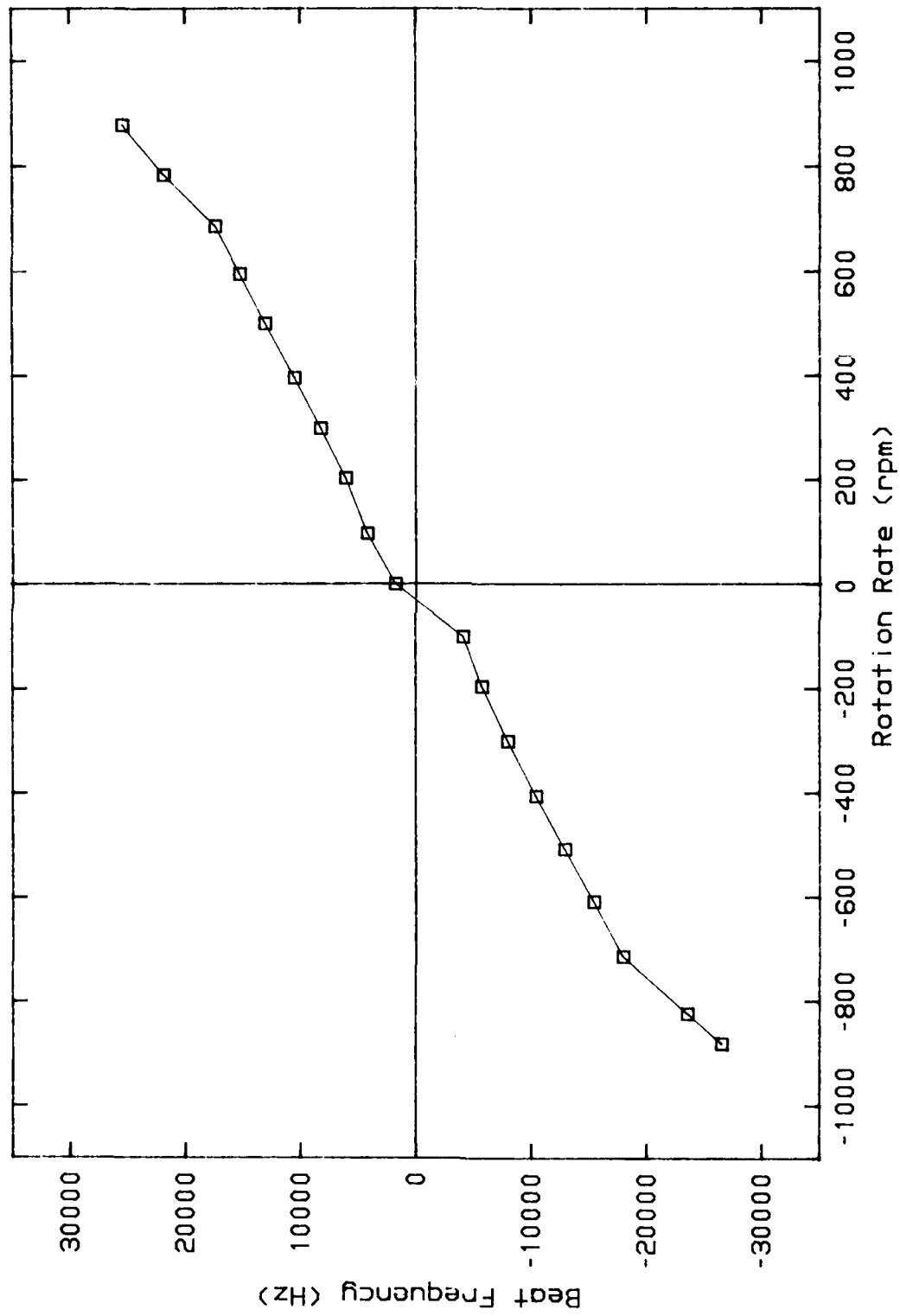
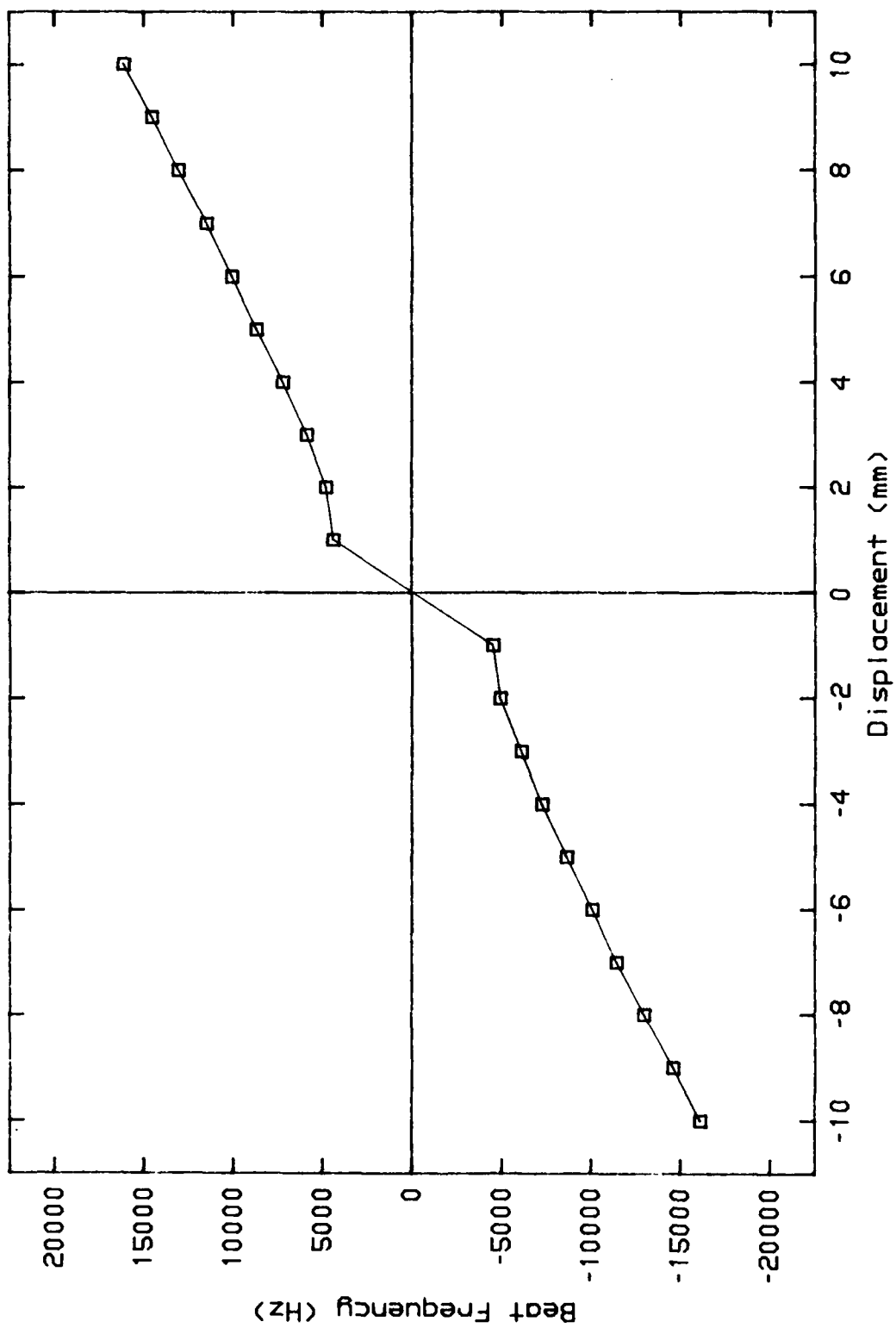Figure 6.1 - Beat Frequency vs Drag Disk Rotation Rate.

Figure 6.2 - Beat Frequency vs Drag Disk Displacement.

CHAPTER VII

SUMMARY AND CONCLUSIONS

From Chapter VI, it can be seen that the results of
this experiment did not turn out as expected. The research
was performed in an effort to determine the Fresnel drag
coefficient, using a ring laser, to a degree of accuracy
higher than had been determined by all previous works.
This was attempted by trying to improve upon the accuracies
with which the parameters, used to determine α, were
measured. The degree of accuracy, in percent, of the
following parameters were increased beyond those of the
Bilger-Stowell experiment: wavelength (λ) by 1250 times,
drag disk thickness (1) by 1.67 times, inclination angle
(β) by 241 times and drag disk displacement (Xo) by 1.4
times. The degree of accuracy, in percent, of the
following parameters equalled those of that previous
experiment: refractive index (n) and dispersion ($dn/d\lambda$).
The degree of accuracy, in percent, of the following
parameters turned out to be less than those of the Bilger-
Stowell experiment: optical path length (L) by 6 times,
rotation rate (f_m) by 10 times and beat frequency (δf_B) by
about 50 times. The accuracies of these last three

parameters can be improved upon and will be covered in the next section. Nonetheless, the accuracies with which the last three parameters were measured do not account for the amount of difference between the experimentally and theoretically determined Fresnel drag coefficient. See tables 6.1 - 6.3 in Chapter VI. Also, the degree of accuracy in the determination of α for this experiment was about 61 times worse than that for the Bilger-Stowell experiment. It is believed, as stated in the previous chapter, that the reason for the low accuracy and the large difference from theory was due primarily to the thickness of the drag disk. Since the wobble of the disk could not be eliminated, the intracavity beam's intensity oscillated as well as the beat frequency signal resulting in a modulation of the beat frequency and a periodic diminishing of the intensity of the signal. The amplitude of the beat frequency signal, at these points, was too low to be detected by the counter. This caused an undercount by the counter.

It is regrettable that time did not allow the examination of all of the shortcomings discovered with this experiment. Several of the suggestions for improvement listed below could have easily been implemented in this experiment had the apparatus necessary to effectuate these improvements been delivered before its conclusion. These suggestions, however, most certainly will be put to the

proof for the surface studies program.

Suggestions For Improvement

It is the belief of this author that the single most important improvement to this experiment would be to acquire a thinner drag and compensation disk. Although a thinner disk would increase the rate in which it would have to be rotated, the effects of wobble could be decreased and thus eliminate the periodic diminishing of the beat frequency signal. With a thinner optical flat, the front and back working surfaces could be polished to a higher degree of parallelism since it is easier to polish a thinner disk to the desired specifications. This would reduce the actual amount of wobble demonstrated by the drag disk and hence further decrease the wobble effects that plagued this experiment. A thinner disk would mean less mass, so the need for the massive air bearing and drive mechanism would not be required. It would also need less gas pressure to float the air bearing reducing the air currents and dust particles around the drag disk. With a much smaller air bearing, a brushless motor could be attached to the bearing itself, driving the disk without the need of a belt. Vibrations due to the belt would thus be reduced, resulting in less noisy system. This would eliminate the need to control the belt tension. A thinner drag disk could allow operation with the contrapropagating

beams near the center of rotation, as refraction of the
beams through the thinner medium would not be as severe as
for the thick disk. This would minimize the effects of the
dust contamination of the flat since dust did not
accumulate on the working surfaces near the center of
rotation of the disk as heavily as it did closer towards
the edges. This, in turn, could allow operation at
Brewster angle. By performing the experiment at Brewster
angle, the laser power would be at a maximum. Conceivably,
this could be enough power to read the beat frequency of
the laser cavity modes, measured for determining the
optical path length, directly by the counter without
attempting to line up the peaks of both the beat frequency
and the signal generator on the spectrum analyzer. See
Chapter IV. Human error could, thus, be eliminated from
this particular measurement and increase its degree of
accuracy. This measurement could further be automated to
record L simultaneously with the beat frequency and the
rotation rate giving an increase in the degree of accuracy
for the determination of the Fresnel drag coefficient. To
actually control the optical path length of the ring laser
cavity a Litton piezoelectric driven mirror, used in
Litton's own ring laser gyroscopes, and a Lansing model
80.215 lock-in stabilizer were acquired. They were never
implemented, however, due to the shortage of time. Path
length control could have ensured a constant path length

throughout the experiment.

The degree of accuracy with which the refractive index was determined could have been improved upon by a direct measurement by Schott Optical Glass, Inc. They perform this measurement to $\pm$ 5 x 10^{-6}. This would render a value of n accurate to within $\pm$ 0.0003%.

The filters used in this experiment, to process the beat frequency signal, did not perform as anticipated. After recording the beat frequency measurements it was deduced that a filter with a very narrow band pass would be desired. Also, for convenience, it would be desirable for the band pass frequency of the filter to have the capability to be computer controlled allowing automation. This could eliminate the need to manually adjust the band pass frequency before each measurement.

Another suggestion for convenience, envisioned after performing this experiment, would be to find or design a housing for the disk that would be narrower than the disk itself to allow easier cleansing with collodion after the disk was in place. The present setup did not allow cleansing out to the edges of the disk as the collodion would flow over the edge, underneath the retainer ring and onto the o-rings that held the disk in place. Also, not being able to coat the disk with collodion out to the edge, there was more of a possibility of scratching the surface of the disk when removing the collodion.

With a configuration utilizing a brushless motor to drive the disk, no belt, the angle indicator and optical encoder could be replaced with a motorized rotation stage inserted under the drag disk mount and a motorized rotation stage could also be inserted under the compensation disk mount. This could allow rotation of both disks about the Z axis and provide the capability to control the inclination angle with the computer. This would insure a more precise angle setting, of both disks, instead of the present procedure of setting the drag disk and then adjusting the compensation disk until lasing occurs. The inclination angle of both disks would have the same high degree of accuracy. This could better insure that both counter-propagating beams were coincident and parallel. In that modified configuration the refraction of the beams would be in the X direction, instead of the Z direction as it was for this experiment.

Looking back on this experiment the characteristics of the ring laser, used in the experiment, were derived from the mirrors that were on hand. It would have been far more desirable to design the mirrors for the ring and specify beam waist diameter, length and position. Mirrors were indeed determined for this ring laser to give a 0.5 mm beam waist diameter with the center of the waist at MM4, the test mirror for the surface studies program. They did not arrive in time for use in this experiment.

The degree of accuracy with which the location of the center of rotation of the drag disk could be determined was explored. One could improve upon its accuracy by use of the operating ring. An algorithm for determination of the center of rotation was developed that closed in on the exact center by use of the beat frequency, rotation rate and approximate displacement of the drag disk. (Berney, 1986). Data taken, at several approximate vertical and horizontal displacements about the face of the disk, and then compared with displacements calculated for a particular beat frequency and rotation rate would give a more accurate location of the center of rotation and thus, give a higher degree of accuracy for Xo. The premise for the use of this algorithm is to have a low noise, properly functioning ring with a below earth rate lock-in frequency. This was not the case for the ring laser used in this instance. It is believed, however, that it could have been with the replacement of several components described above such as mirrors, filters and optical flats.

APPENDIX A

THERMAL EXPANSION

Considerations

Thermal expansion was one of the concerns when designing the ring laser gyroscope for this experiment. The most important component of the ring laser gyro was the resonant cavity itself. Thermal instabilities of the materials making up the mirror mounts could alter the optical path length, introducing error into the measurements for the Fresnel drag coefficient.

The table tops, bases, mirror mounts, and the mounts used for the drag and compensation disks were made from invar, stainless steel, and Al (aluminum). These metals have coefficients of thermal expansion of $1.44 \times 10^{-6}/^{\circ}K$, $9.6 \times 10^{-6}/^{\circ}K$, and $23.4 \times 10^{-6}/^{\circ}K$, respectively. For a worst case analysis we will consider the thickest horizontal dimension of the Al bases to which the mirror mounts were attached. This dimension was measured to be 120 mm. A $5^{\circ}K$ variation from one side of each base to the next, which was far worse than could be maintained, would produce a change of only 7 μm in the horizontal position of the mirror face. If all four mounts experienced this

71

temperature gradient, the total change in position, and hence path length, would amount to 28 μm. The accuracy with which the path length was measured in this study was 0.006% or $\pm$ 236 μm. See Chapter IV. Therefore, the contribution of error from the thermal sensitivities of the metals used was neglected.

APPENDIX B

RING LASER CAVITY ALIGNMENT

An accurate description of the mounts, translation
stages, and bases making up the ring laser cavity will be
discussed as well as an account of the alignment procedures
applied.

Components

The majority of the translation stages and mirror
mounts making up the ring laser cavity were manufactured by
KS (Klinger Scientific). Mirror mounts MM1-MM3 were made
up of one model SK 25.4BM mirror mount, two model MR 80.25
horizontal translation stages positioned perpendicular to
each other for movement along the X and Y axes, one model
TR 80 rotational stage for rotation about the Z axis, and
one model MV 80 vertical translation stage for movement
along the Z axis. Each set of components were attached
together and mounted onto an Al (aluminum) base. See
figure B1. The Al bases brought the laser cavity mirrors
up to, approximately, the reference height established by
the height of the mount configuration for the drag disk.
The rotational stage was mounted below the horizontal

stages in order to position the face of the mirrors at the center of rotation about the Z axis. The Al bases were fixed to the NRC invar breadboard atop the NRC vibration isolation table.

Mirror mount MM4 was made up of one model SK 25.4BM mirror mount fixed to two model UT 100.25 motorized translation stages mounted perpendicular to each other to provide movement along the Z axis and, depending on the rotational orientation of the mirror about the Z axis, movement in the X or Y direction or in both the X and Y direction. See figure B2. These stages were attached to a model RT 200 motorized rotation stage with the rotational axis perpendicular to Z. The mirror mount configuration was encased in an aluminum framework to provide support for the weight of the stages. The framework was mounted to a model MR 160.8C horizontal translation stage to provide X or Y or both X and Y translation depending on the rotational orientation about Z. This was fixed to a model TR 160 rotation stage to provide rotation about the Z axis. As with the other mirror mounts, the rotation stage making up MM4 was attached beneath the horizontal translation stage to allow positioning of the face of the mirror to the center of rotation. This configuration was secured to an Al base anchored to the invar breadboard. Although used over the course of this experiment, the motorized stages and large framework making up MM4 were not required but

were included for a parallel effort investigating laser gyro mirror surfaces.

Both ends of the laser gain tube were secured in a delrin holder that clamped around tube. Each delrin holder was mounted to a model MV 80 vertical translation stage for translation along Z and a model MR 80.25 translation stage for translation along X. This setup was mounted to an Al base and fastened to the invar breadboard. See figure B3. The Al base was large enough to accommodate the three lengths of the laser tubes tried during this experiment.

Alignment Procedures

Refer to figure 3.1, Chapter III, for a layout of the ring laser components. Mirrors M1-M4 would be secured into mirror mounts MM1-MM4, respectively. Starting with all mounts vacant, the translation stages making up MM1-MM4 were centered according to their micrometer readings. A delrin pinhole was placed into MM4. Using a Mitutoyo model 192-606 height gage, the distance from the top of the invar breadboard to the center of the pinhole was measured to within 0.001". This was used as the reference for adjusting the heights of the other mirror mounts. The pinhole was placed in MM1-MM3 and the heights of these mounts were set to the reference by adjusting the model MV 80 vertical translation stages attached to these mounts.

After positioning the heights, pinholes were inserted

into MM1 and MM2. The model TR 80 rotational stages on
these mounts were rotated about the Z axis until the
pinholes were facing each other and normal to the alignment
laser beam. The Lansing model 39.102 VPB alignment laser,
positioned behind MM1, was adjusted following Lansing's
instruction manual until the laser beam passed through both
pinholes without any distortion. MM1 was positioned so
that the front reflecting surface of M1 would be at the
center of rotation when inserted into the mount. This was
accomplished by rotating the TR 80 rotation stage, on MM1,
back and forth by 180° from normal in both directions about
Z to make sure that the laser illuminated the pinhole
throughout the entire rotation. The two model MR 80.25
translation stages on MM1, the X and Y translation stages,
as well as the alignment laser behind MM1 were adjusted
until this was observed. The pinhole was removed from MM1
and the same procedure was applied to MM2. The pinhole was
then placed back in MM1 and the process was repeated. This
continued until the pinholes in both mounts remained
illuminated over the 360° rotation. The alignment laser
would not be adjusted again throughout the remainder of the
alignment procedure. The TR 80 stages on MM1 and MM2 were
once again rotated about Z until the pinholes were facing
towards each other and normal to the alignment laser beam.

The plasma tube was placed in its mount, ignited, and
allowed to warm up for about an hour. It was found that an

hour warm up was necessary to allow the temperature of the tube to stabilize before alignment as the tube tended to shift as it heated up. Using the translation stages that made up the mount, the tube was then positioned so that the alignment laser passed through the excited plasma tube and both pinholes without any distortion to the beam.

The TR 80 rotation stage on MM2 was locked in place, facing MM1 and perpendicular to the alignment laser beam. Mirror M2 was secured into MM2 and the tilt micrometers on the model SK 25.4BM fixed to MM2 were set to reflect the alignment laser back onto itself. The pinhole that was removed from MM2 was placed in MM3. The TR 80 rotation stage on MM3 was rotated about Z until the pinhole faced MM2 and was perpendicular to the alignment laser beam. The TR 80 on MM2 was unlocked, rotated 45° ccw (counter clockwise) about the Z axis, until the pinhole at MM3 was illuminated, and again locked in position. The center of rotation for MM3 was determined in the same way as it had for MM1 and MM2 but without any adjustments made to either the alignment laser or to the other two mounts. Only the model MR 80.25 X and Y translation stages on MM3 were adjusted. After finding the center of rotation, the TR 80 rotation stage on mount MM3 was again rotated about Z until the pinhole faced MM2 and was normal to the alignment laser beam. MM3 was locked in place.

Mirror M3 was secured into MM3 and the tilt micrometers

on the SK 25.4BM fixed to MM3 were adjusted until the
alignment laser was reflected back onto itself. The
pinhole, removed from MM3, was then placed in MM4 and the
model TR 160 rotational stage on MM4 was rotated about Z
until it faced MM3 and was normal to the alignment laser
beam. The TR 80 on MM3 was unlocked, rotated 45° ccw about
Z so that the pinhole at MM4 was illuminated by the
alignment laser, and again locked in place. The TR 160 on
MM4 was rotated about the Z axis to find the center of
rotation. Due to the logistics of this mount, the pinhole
could only be rotated back and forth by about 60° from
normal in either direction. The model MR 160.80 horizontal
translation stage on MM4 was adjusted until the pinhole
remained illuminated throughout the 120° of possible
travel. The TR 160 on MM4 was rotated until the pinhole
was again facing MM3 and perpendicular to the alignment
laser beam. It was then locked in place.

Mirror M4 was secured into MM4 and the tilt micrometers
on the SK 25.4BM attached to MM4 were set so that the
alignment laser was reflected back onto itself. The TR 80
rotation stage on MM1 was locked in place so that the front
face was in the direction of MM2 and normal to the
alignment laser beam. Mirror M1 was then secured into MM1.
The tilt micrometers on the SK 25.4BM fastened to MM1 were
adjusted until lasing occurred between M1-M4.

Next, the HLBA (Hughes laser/beamsplitter assembly) was

horizontally translated into the laser cavity between MM1
and the Brewster window of the plasma tube. It reflected
the laser into the cavity towards M2. This was
accomplished with the beamsplitter assembly which included
a Melles Griot model 03BPL003/02 pellicle with
approximately a 50/50 reflection/transmission ratio at a
wavelength of 632.8 nm. The beamsplitter assembly provided
translation, tilt, and rotation to allow adjustment of the
direction of travel of the beam from the Hughes laser. The
assembly was adjusted until the reflection of the HLBA from
the mirrors went back into itself. This assured that the
HLBA was aligned and normal to the ring cavity.

The TR 80 on MM1 was unlocked, rotated 45° cw
(clockwise) about Z and again locked in place. The TR 160
on MM4 was unlocked, rotated 45° ccw and locked in place.
The tilt micrometers of the SK 25.4BM on MM1 were adjusted
until the HLBA was reflected back onto itself. All mirrors
were now at a 45° angle of incidence to the direction of
the beam of the HLBA and hence, the ring laser cavity. The
HLBA was translated out of the ring cavity and lasing
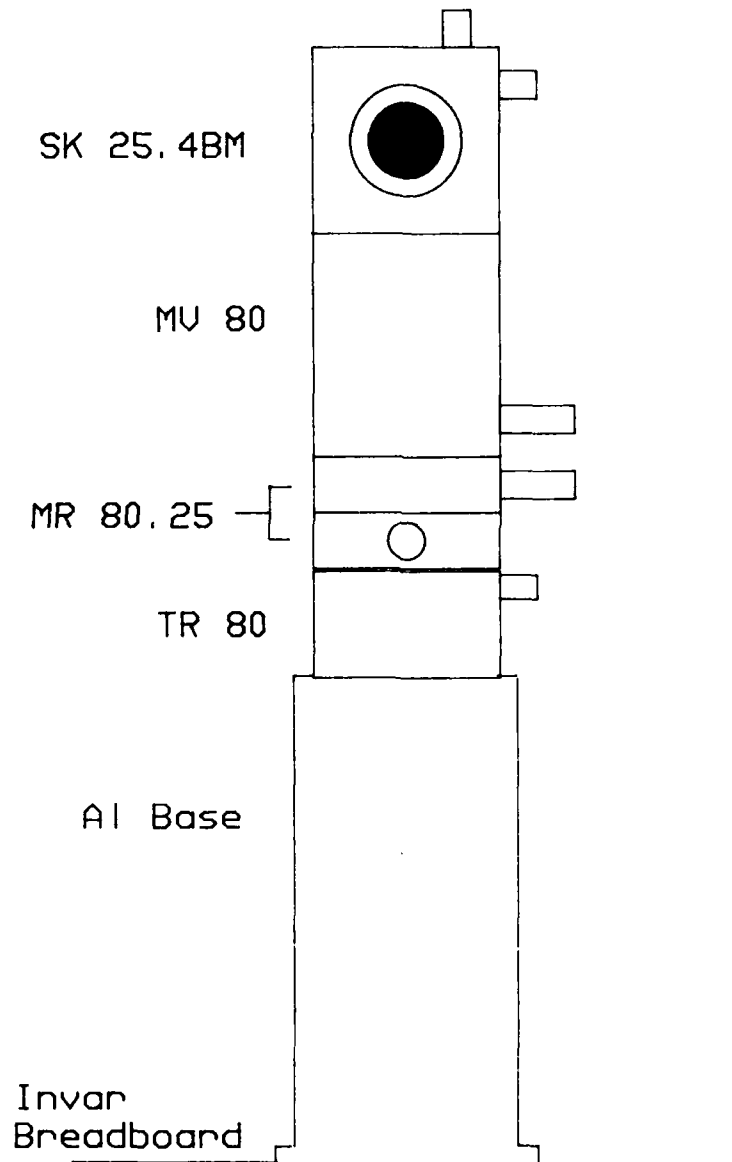occurred when the assembly cleared the cavity.

SK 25.4BM

MV 80

MR 80.25

TR 80

Al Base

Invar
Breadboard

Figure B1 - Mirror Mount Assembly for Mirrors M1, M2 and M3.

81

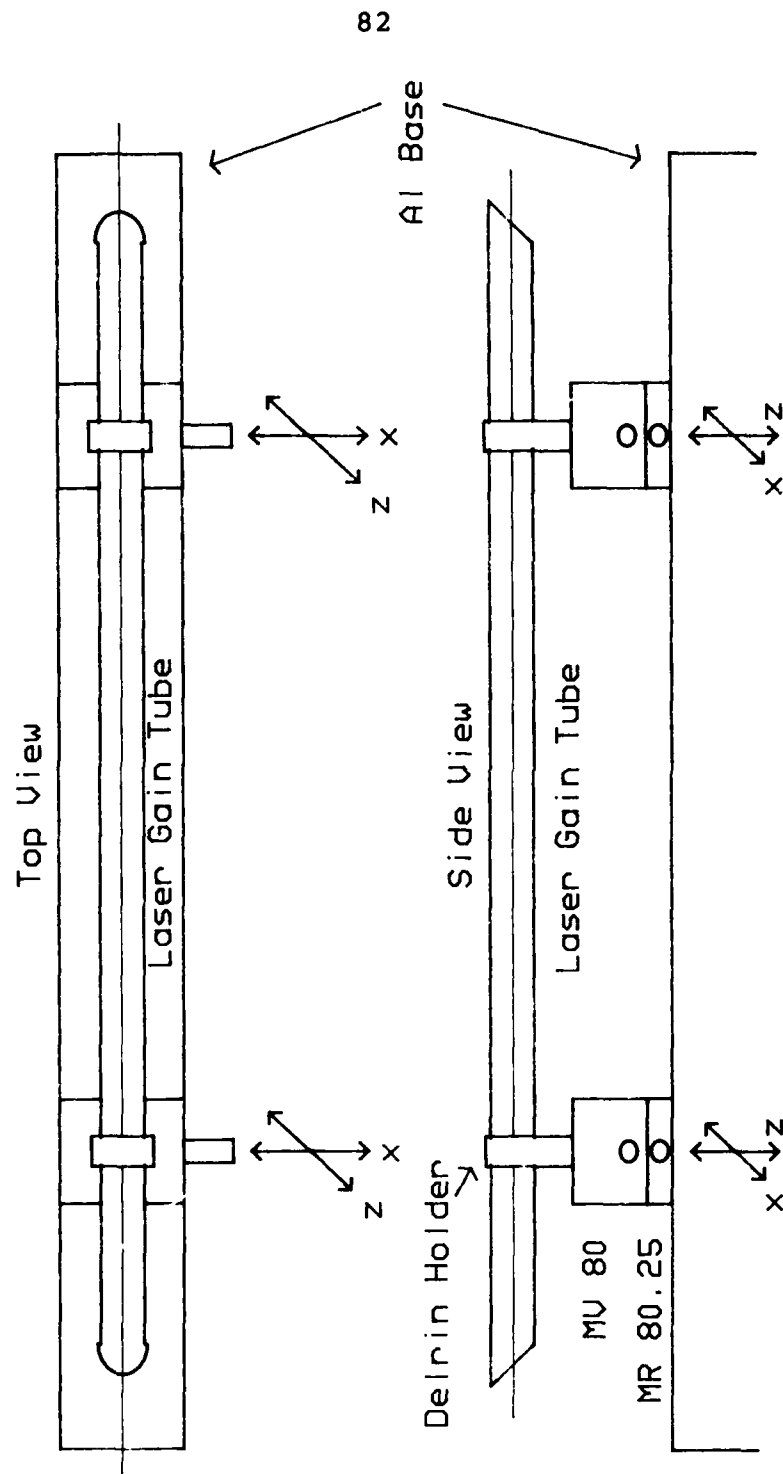Figure B2 - Mirror Mount Assembly for Mirror M4.

Figure B3 - Laser Gain Tube Mount.

APPENDIX C

DISK DRIVE BELT TENSION ANALYSIS

The tension of the drive belt used to rotate the drag disk greatly affected the position of the center of rotation of the disk with respect to the intracavity laser beam. It was observed that as the tension of the belt increased, the position of the center of rotation shifted closer towards the motor driving the disk, and as the belt tension decreased, the position of the center of rotation shifted in the opposite direction.

The position of the center of rotation of the disk was measured for various belt tensions and at various rotation rates, following the procedure outlined in Chapter IV using the torque watch gage and the ruler. The rotation rate of the disk ranged from 100 rpm to 2000 rpm. It was discovered that the rotation rate did not affect the position of the center of rotation of the disk. The position remained the same throughout the entire range of rotation rates. It is believed that this is due to the fact that the air bearing used exhibited minimal friction, so did not add to the torque. The tension of the drive belt was varied from 0.05 oz. to 1.2 oz.

Figure C1 illustrates the effect for the various belt tensions. Figure C1 is a plot of the amount of shift in the position of the center of rotation of the drag disk versus the amount of tension in the drive belt. From this graph it is readily seen that it was very important to maintain a constant belt tension throughout the measurements of the parameters used to determine the drag coefficient. Because the rotation rate did not alter the position of the center of rotation, the belt tension required measurement only prior to making data runs or if the drag disk was translated during a data run where the tension might have to be readjusted as well.
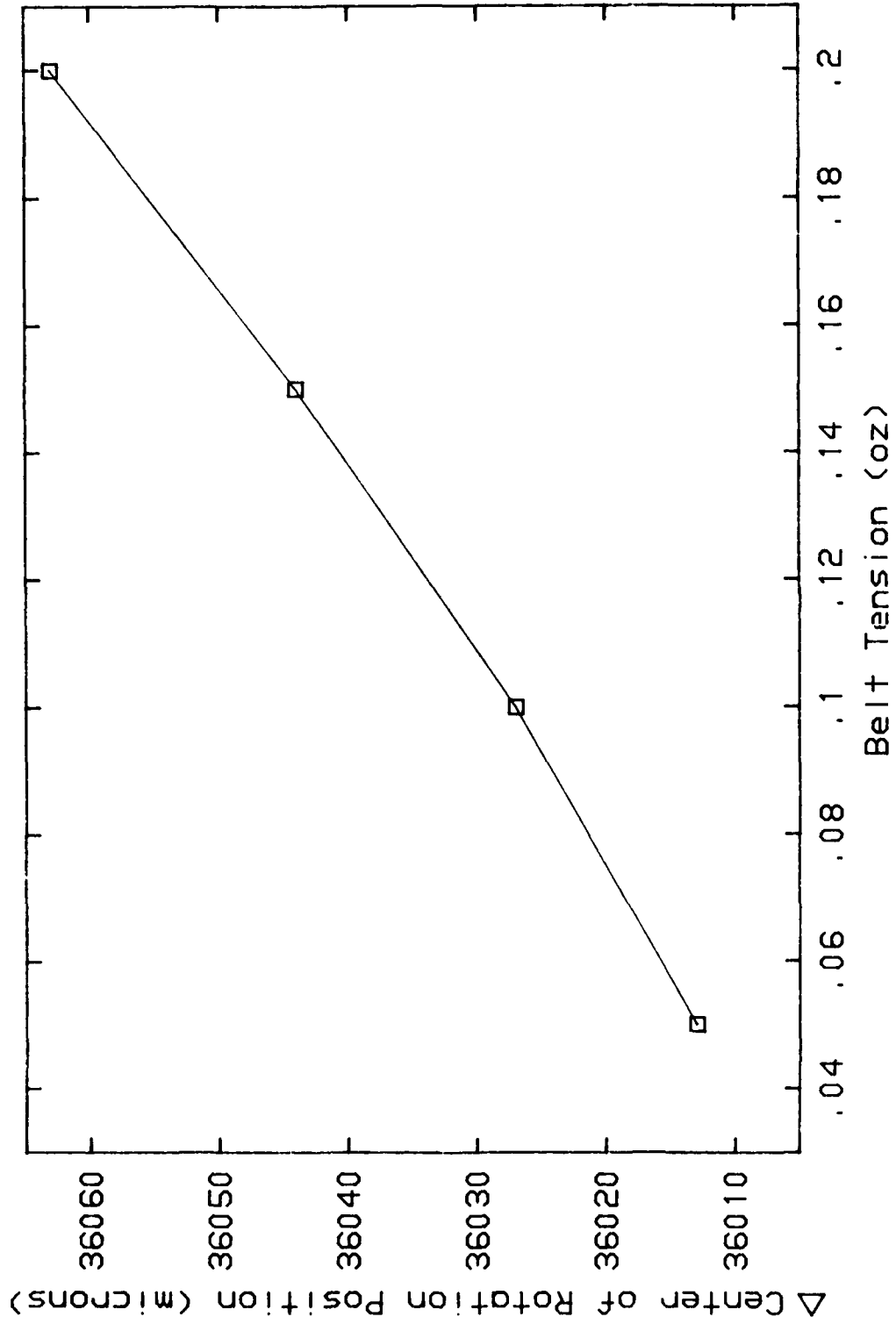
Figure C1 - Drag Disk Center of Rotation Position vs Drive Belt Tension.

BIBLIOGRAPHY

Heraeus Amersil Data Brochure, (1981).

R. Berney, Developed an algorithm and computer program that could determine the center of rotation of the drag disk installed in the ring laser cavity. This was performed while he was working on the ring laser test bed project as part of a summer research program at Wright-Patterson Air Force Base, 1986.

H. R. Bilger and A. T. Zavodny, "Fresnel Drag in a Ring Laser: Measurement of the Dispersive Term," _Physical Review A_, Vol. 5, No. 2, 591, (February, 1972).

H. R. Bilger and W. K. Stowell, "Light Drag in a Ring Laser: An Improved Determination of the Drag Coefficient," _Physical Review A_, Vol. 16, No. 1, 313, (July, 1977).

G. Birnbaum, _Optical Masers_, Academic Press, New York, NY, 1964.

M. Born and E. Wolf, _Principles of Optics_, Sixth edition, Pergamon Press, New York, NY, 1986.

S. Chao, W. L. Lim and J. A. Hammond, "Lock-in Growth Rate in a Ring Laser Gyro," _SPIE Proceedings, Physics of Optical Ring Gyros_, 487, 50, (1984).

W. W. Chow, J. Gea-Banacloche, L. M. Pedrotti, V. E. Sanders, W. Schleich and M. O. Scully, "The Ring Laser Gyro," _Reviews of Modern Physics_, Vol. 57, No. 1, 61, (January, 1985).

A. Garscadden, AFWAL/POOC-3, Wright-Patterson Air Force Base, OH, Private conversations, (1986).

Handbook of Chemistry and Physics, R. C. Weast, Editor, Sixty-Sixth edition, CRC Press, Boca Raton, FL, 1985-1986.

E. Hecht and A. Zajac, _Optics_, Addison-Wesley Publishing Company, Reading, MA, 1974.

C. V. Herr, "History of the Laser Gyro," SPIE Proceedings, Physics of Optical Ring Gyros, 487, 2, (1984).

F. A. Jenkins and H. E. White, Fundamentals of Optics, Fourth edition, McGraw-Hill, New York, NY, 1976.

J. E. Killpatrick, "The Laser Gyro," IEEE Spectrum, 44, (October, 1967).

M. V. Klein, Optics, John Wiley and Sons, New York, NY, 1970.

H. Kogelnik, "Imaging of Optical Modes--Resonators with Internal Lenses," The Bell System Technical Journal, 19, 455, (1964).

M. v. Laue, "Die Mitführung des Lichtes durch bewegte Körper nach dem Relativitätsprinzip," Annalen der Physik, 23, 989, (1907).

H. A. Lorentz, The Theory of Electrons and its Applications to the Phenomena of Light and Radiant Heat, Second edition, Dover Publications, New York, NY, 1952.

W. M. Macek, J. R. Schneider and R. M. Salamon, "Measurement of Fresnel Drag with the Ring Laser," Journal of Applied Physics, 35, 2556, (1964).

A. A. Michelson, Studies in Optics, The University of Chicago Press, Chicago, IL, 1962.

Official Geographic Coordinates Survey Field Book, Wright-Patterson Air Force Base Surveyors, Wright-Patterson Air Force Base, OH, (1986).

D. C. O'Shea, W. R. Callen and W. T. Rhodes, Introduction to Lasers and Their Applications, Addison-Wesley Publishing Company, Reading, MA, 1978.

W. F. Parks and J. T. Dowell, "Fresnel Drag in Uniformly Moving Media," Physical Review A, Vol. 9, No. 1, 565, (January, 1974).

T. J. Podgorski and F. Aronowitz, "Langmuir Flow Effects in the Laser Gyro," IEEE Journal of Quantum Electronics, Vol. QE-4, No. 1, 11, (January, 1968).

E. J. Post, "Sagnac Effect," Review of Modern Physics, 39, 475, (1967).

W. W. Rigrod, "The Optical Ring Resonator," The Bell System Technical Journal, 907, (1965).

W. S. Rodney and R. J. Spindler, "Index of Refraction of Fused-Quartz Glass for Ultraviolet, Visible and Infrared Wavelengths," Journal of Research of the National Bureau of Standards, 53, 185, (1954).

M. Sargent III, "Basic Ring Laser Gyro Theory," SPIE Proceedings, Physics of Optical Ring Gyros, 487, 22, (1984).

A. E. Siegman, An Introduction to Lasers and Masers, McGraw-Hill, New York, NY, 1971.

W. K. Stowell, "A Precision Measurement of Fresnel Drag in a Ring Laser," Unpublished PhD. Thesis, Oklahoma State University, Stillwater, OK, (1974).

W. K. Stowell, AFWAL/AADO-2, Wright-Patterson Air Force Base, OH, Private conversations, (1985-1986).

A. R. Striganov and N. S. Sventitskii, Tables of Spectral Lines of Neutral and Ionized Atoms, Plenum Press, New York, NY, 1968.

J. S Uppal, J. C. Monga and D. D. Bhawalkar, "A Simple Technique for the Alignment of a Ring Resonator," Optics and Laser Technology, 215, (August, 1985).

A. Yariv, Quantum Electronics, Second edition, John Wiley and Sons, New York, NY, 1975.

A. Yariv, Optical Electronics, Third edition, Holt, Rinehart and Winston, New York, NY, 1985.

P. Zeeman, "Fresnel's Coefficient for Light of Different Colours-First Part," Proceedings of the Royal Academy of Amsterdam, 17, 445, (1914).

P. Zeeman, "Fresnel's Coefficient for Light of Different Colours-Second Part," Proceedings of the Royal Academy of Amsterdam, 18, 338, (1915).